

AD-A230 586

DTIC FILE COPY

(1)



DTIC

ELECTED
JAN 07 1993

D

DEPARTMENT OF THE AIR FORCE INSTITUTE OF TECHNOLOGY

DISTRIBUTION STATEMENT A

Approved for public release
Distribution Unlimited

DEPARTMENT OF THE AIR FORCE
AIR UNIVERSITY
AIR FORCE INSTITUTE OF TECHNOLOGY

Wright-Patterson Air Force Base, Ohio

91 1 3 119

AFIT/GSO/ENS/90D-12

61

DTIC
ELECTED
JAN 07 1991
S D
D

DEVELOPMENT OF AN IMAGE REGISTRATION
TECHNIQUE FOR POLAR-ORBITING SATELLITES

THESIS

Jerry L. Mehlberg, Captain, USAF

AFIT/GSO/ENS/90D-12

DISTRIBUTION STATEMENT A
Approved for public release
Distribution Unlimited

Approved for public release; distribution unlimited

DEVELOPMENT OF AN IMAGE REGISTRATION
TECHNIQUE FOR POLAR-ORBITING SATELLITES

THESIS

Presented to the Faculty of the School of Engineering
of the Air Force Institute of Technology

Air University

In Partial Fulfillment of the
Requirements for the Degree of
Master of Science in Space Operations

Jerry L. Mehlberg, B.S.

Captain, USAF

December 1990

Accepted For	J
NTIS	CP441
DDIC	TE63
Unpublished	
Justification	
By	
Distribution	
Average	
Dist	A-1
	Approved
	for public release
	unlimited

A-1

Approved for public release; distribution unlimited

THESIS APPROVAL

STUDENT: Jerry L. Mehlberg CLASS: GSO-90D

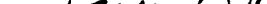
THEESIS TITLE: Development of an Image Registration
Technique for Polar-Orbiting Satellites

DEFENSE DATE: 30 Nov 90

COMMITTEE: NAME/DEPARTMENT SIGNATURE

Advisor/co-Advisor Thomas S. Kelso 
(circle appropriate role)

co-Advisor/ENS Representative _____

Reader James N. Robinson 

Preface

The purpose of this paper is to improve and to simplify the geographical registration of TIROS-N satellite images. This work is a follow-up on a technique proposed by Larcomb in 1989. The power of this technique comes from its independence from using ground control points. This capability is imperative over oceans, deserts, or any area lacking easily identifiable points. In this thesis I took his work through the next logical steps. First, I expanded his algorithm to include worldwide coverage. Then, it was subjected to a series of tests to establish a level of confidence in its accuracy. Finally, a program structure was developed, allowing its use on different types of computer systems.

This project is greatly indebted to the work of Larcomb for which I am very thankful. His compilation of knowledge from various sources along with providing the initial Pascal source code for the process made a perfect springboard from which to start. I am grateful for the help and guidance I received from Dr. Thomas S. Kelso. His long hours of image collection, and his display programs, gave me needed tools to work with. I would like to thank my wife Rose, and my daughters, Jessica and Jacqueline, for their support and for the enthusiasm they expressed in this project.

Jerry L. Mehlberg

Contents

	Page
Preface	ii
List of Figures	v
List of Tables	vi
List of Symbols	vii
List of Equations	viii
Abstract	xi
I. Introduction	1
Background	1
Problem Statement	5
Scope	5
Assumptions	5
Objectives	6
Definitions	7
II. Historical Development	10
Works Prior to Larcomb	10
Larcomb's Model	11
Validation and Sensitivity Analysis	16
III. Modifications to Larcomb's Algorithm	19
Orbital Mechanics	19
Viewing Geometry	20
Direct Referencing	21
Inverse Referencing	22
IV. Methodology	28
Modular Program Design	28
Verification	31
Validation	32
Measures of Performance	37
Sensitivity Analysis	37
V. Results and Discussion	39
Verification	39
Validation	41
Sensitivity Analysis	55

Contents

VI. Conclusions and Recommendations	69
Conclusions	69
Recommendations	71
Appendix A: Ref Unit	72
Appendix B: Support Units	74
Appendix C: Verification Test Programs	77
Appendix D: APT-RVW2 Program	79
Bibliography	80
Vita	81

List of Figures

Figure	Page
1. Generalized Inverse Referencing	23
2. Data Flow	29
3. Checkpoints Used for Validation	34
4. Image of Eastern United States	43
5. Registered Image of Eastern United States . . .	44
6. Regression Analysis of Minute Mark Drift . . .	50
7. Regression Plot of Observed Errors	54
8. Registration With No Errors	59
9. +3.0 Degree Pitch Error	60
10. +3.0 Degree Roll Error	61
11. +3.0 Degree Yaw Error	62
12. +0.09 Rev/Day Mean Motion Error	63
13. +0.004 Eccentricity Error	64
14. +2.0 Degree Ascending Node Error	65
15. +2.0 Degree Inclination Error	66
16. -10.0 Second Image Time Error	67
17. Registered Image With Satellite Yaw Error . . .	68

List of Tables

Table	Page
1. Direct Referencing Statistics	46
2. Inverse Referencing Statistics	46
3. Epoch and Minute Mark Statistics	47
4. Regression Analysis for Cross-Track Errors . . .	51
5. Regression Analysis for Along-Track Errors . . .	52

List of Symbols

Symbol	Meaning
i	The angle between the satellite ground track and the equator. In some cases, this angle will be the same as the satellite's inclination.
j	The angle between the equator and the great circle through the nodal point and earth location.
r	The satellite's orbital radius.
t_N	The nodal crossing time.
v_z	The satellite's component of velocity in the polar direction.
β	The earth centered angle between the nodal crossing point and the earth point.
θ	The earth-centered angle between the nodal point and the midpoint.
θ'	The first time derivative of θ .
λ_S	The subpoint static longitude.
λ_N	The nodal point longitude.
μ	The earth's gravitational constant.
ϕ_S	Latitude of the subpoint.
ψ	The earth center angle between the satellite's subpoint and the earth location.
Ω'	The orbital precession rate.
ω	The earth's rotation rate.

List of Equations

$$\sin \theta_S = \sin \Phi_S / \sin i \quad (1)$$

$$\theta' = ge / r^3 \quad (2)$$

$$t_N = t_S - \theta_S / \theta' \quad (3)$$

$$\cos \lambda_S = \cos \theta_S / \cos \Phi_S \quad (4)$$

$$\lambda_N = \lambda_S + \lambda'_S + (t_S - t_N)(\omega - \Omega') \quad (5)$$

$$\sin j = \sin \Phi_E / \sin \beta \quad (6)$$

$$\sin \psi = \sin(j-i) \sin \beta \quad (7)$$

$$\begin{aligned} -0.884 \text{ CRT pixels} &= -1.15 \text{ APT pixels} = -4.0 \text{ km} \\ &= -0.0009 \text{ radian longitude} \end{aligned} \quad (8)$$

$$\begin{aligned} 0.0647 \text{ CRT lines} &= -0.0647 \text{ APT lines} = -0.21 \text{ km} \\ &= -0.00004 \text{ radian latitude} \end{aligned} \quad (9)$$

$$1.25 \text{ APT combined pixels} \approx \text{one CRT pixel} \quad (10)$$

$$\begin{aligned} 1.3 \text{ CRT pixels} &\approx 1.6 \text{ combined APT pixels} \\ &\approx 5.5 \text{ km} \end{aligned} \quad (11)$$

Abstract

In this study, a means to perform spatial registration (gridding) of meteorological satellite data is developed. It is applicable to Automatic Picture Transmission (APT) data from the TIROS-N series polar-orbiting satellites operated by the National Oceanic and Atmospheric Administration (NOAA). This technique does not require the use of ground control points. Registration is accomplished using an advanced orbital model to precisely compute the satellite's location based on NORAD two-line element sets and the time of the image. This technique is examined for accuracy and sensitivity to errors in the element set and satellite attitude control. This study involves over 70 images over a 60-day period.

DEVELOPMENT OF AN IMAGE REGISTRATION
TECHNIQUE FOR POLAR-ORBITING SATELLITES

I. Introduction

Background

While meteorological satellites have been orbiting the earth for many years, only recently has receiving technology been available to the public at large. The reception of images from space by private individuals and groups has created an entirely new aspect to the "information age." Besides weather data, meteorological satellites have been providing data for oceanographic, land use, earth sciences education, and other purposes. Additional uses for meteorological satellite data will be found as direct broadcast of data becomes more widespread.

The Television Infrared Observation Satellite (TIROS-N) is a meteorological spacecraft operated by the United States that transmits a continuous stream of data to any radio capable of receiving it. This data is 'video raster information consisting of radiometric measurements of surface and cloud features. It transmits imagery gathered by visual and infrared sensors at a low data rate, allowing it to be acquired by low-cost receivers. Using a personal

computer, the captured data can be converted into a picture displayable on the computer's monitor.

Observations from space of the earth's surface and atmosphere can provide coverage over a large area. For polar-orbiting satellites this area varies continuously. This is because of the nature of the satellite's orbit. The result -- it is often difficult to determine the exact location of the observations. The varying perspective of the image makes comparisons of them over a period of time difficult. Fixed regions of the earth may appear in different positions and of different sizes in a sequence of images. When geographically identifiable features are missing from the view, such as at night, over the ocean, or when clouds obscure much of the terrain, accurate location information is difficult or impossible to obtain. These problems can limit the usefulness of polar-orbiting satellite data.

The imagery sent by TIROS-N contains no information regarding the geographic location of the pixels. A computer algorithm was developed by Larcomb [3:71-74] to calculate the geographic coordinates of the pixels when given information about the satellite's orbit and the time of data collection. He also laid the groundwork for a means to determine which pixel in an image corresponds to a given geographic location (the inverse to finding the location of a pixel). As indicated by the above discussion, the ability to accurately register (often called "gridding") polar

satellite images can greatly add to the value of the data received from them. If such an algorithm can be incorporated into a program that will operate on a personal computer, many new users of direct readout satellites will benefit from it.

Unlike most registration techniques in current use, Larcomb's algorithm does not require ground control points (GCPs). GCPs are earth locations with known position and are identifiable in the image. The use of GCPs requires an operator to visually identify many such points before registration can be accomplished. This makes registration impossible over oceans and difficult when GCPs are obscured by clouds. Not requiring GCPs is a significant improvement in the process.

Larcomb's algorithm must be validated to ensure its accuracy. This is necessary before it can be useful for serious meteorological, oceanographic, land use, or intelligence data collection.

Several factors limit the accuracy of Larcomb's algorithm. Since this technique is dependent on being able to determine the satellite's position at any moment, the satellite orbital parameters must be known to a high degree of accuracy. Also, the exact time that the data was received is needed. Finally, the satellite's operation, in particular its attitude control and scanning systems, can affect accuracy.

Since these factors can influence the accuracy of the registration, it is important to establish the general accuracy of the algorithm under normal operational circumstances. Establishing accuracy is necessary for any system that makes measurements. A registration program is a system to measure the geographical location of pixels imaged by satellites.

Once the performance of the algorithm has been established, and when the accuracy of the orbital parameters and the timing can be determined, any differences between the calculated locations and the actual locations may be attributed to atypical satellite operation. This may provide a means to determine some of the conditions that the satellite is being operated under. For example, 'errors' in attitude control may be determined by statistical analysis of errors in registration of known ground checkpoints. The ability to extract information from statistical data derived from downloaded satellite data will be useful for several reasons. One reason would be to evaluate the condition of a satellite. Statistical data might be used to detect signs of wear or minor malfunctions before other methods could. Increased registration accuracy might be achieved by being able to measure, and compensate for, periodic and secular tendencies.

Problem Statement

The purpose of this thesis is to extend Larcomb's algorithm to provide worldwide coverage, to create and test a computer program to accomplish registration, to establish its operational accuracy, and to analyze how errors in orbital parameters, timing, and spacecraft operations can affect registration accuracy.

Scope

Although Larcomb's algorithm is equally capable of registering High Resolution Picture Transmission (HRPT) data, this effort will be limited to Automatic Picture Transmission (APT) data since equipment to receive HRPT data is not yet available to the researcher. The registration technique could also be applied to other satellites such as the Defense Meteorological Support Program (DMSP) satellite, but this will not be discussed in this thesis.

Assumptions

A basic assumption made by both Larcomb and this author is that the time of data acquisition by the satellite can be accurately established. As of 8 August 1990, the Manipulated Information Rate Processor (MIRP) minute marker found in the APT raster data can be used to establish this timing [6:5]. Since the data used in this thesis was acquired before this date, the time was established manually (by inspection; see Chapter V). While this may appear to

weaken the results concerning along-track accuracy, this is not the case. In practice, it is fairly easy to obtain timing precision of 0.5 seconds from either the minute marks or by other means. It will be shown that registration errors due to timing are insignificant if the timing error is less than 0.5 seconds. Manual timing determination does not affect the cross-track accuracy calculations. This is demonstrated in Chapter V; see Figure 16. An additional assumption made for the validation test, is that satellite systems and the download equipment are operating correctly (this ensures that the coordinate conversions are done correctly). No assumptions will be made regarding the satellite element sets, therefore the outcome obtained may include effects caused by errors in these element sets. Therefore, the results could be considered to be that obtained under actual operational conditions.

Objectives

The main objective of this study is to validate the registration algorithms proposed by Larcomb for use with the National Oceanographic and Atmospheric Administration (NOAA) polar-orbiting satellites and to establish a level of accuracy. In order to accomplish these objectives, the following sub-objectives will be met:

First, write a Pascal program to conduct registration of APT data. This program is an adaptation of a demonstration program written by Larcomb. The structure of

this code will be modular so that it can be adaptable to a variety of systems. Registration can be accomplished without regard to satellite data capture technique, file formats, or display formats. In addition to registration procedures, graphically oriented code to display images suitable for accuracy measurements, and support functions to interface the registration procedure will be developed.

Second, verify that the code carries out Larcomb's algorithm as closely as possible except where necessary improvements are incorporated by the author.

Third, conduct validation of the program mentioned above over a number of trial runs. Enough samples will be needed in order to assure that anomalies will be detectable. This data should be a collection of error measurements between registration results and "known" geographical positions. A large number of easily identifiable points should be chosen in order to nullify possible map error.

Fourth, do a sensitivity analysis for various aspects affecting registration accuracy.

Lastly, develop corrections, where possible, for errors due to assumptions, implementation, or other factors.

Definitions

Several terms will be used throughout this thesis with specialized meaning. These terms warrant special attention since well defined standards in this area are not yet available or are not widely known.

APT coordinate

A position in APT raster data defined by APT line and pixel numbers. APT lines are relative to the first line in an image. APT pixels are numbered sequentially, starting from the beginning of the scan line and range from 0 to 909.

Calculated ground location

A geographical (geodetic) location calculated by the direct referencing procedure.

Calculated screen position

A position on the CRT screen calculated by the inverse referencing procedure.

Checkpoint

A location on the earth's surface assumed to have known geographical coordinates. Checkpoints are not used as GCPs, they are used only to check registration accuracy.

CRT coordinate

A position on the computer monitor's screen defined by CRT line and pixel number. Normally, line zero is at the top of the screen with the first pixel positioned on the left side, that is, (0,0) is the upper-left-hand corner of the screen.

Geographical coordinate

A set of coordinates that identify a location on the earth's surface in terms of geodetic latitude and longitude.

Ground truth

A checkpoint's true location as determined by measurement on Defense Mapping Agency navigation charts.

Location

Normally refers to a geographic (geodetic) coordinate on the earth's surface, (also see Position).

Midpoint

A subpoint located in the center of the CRT image area.

Position

Normally refers to either a CRT (screen) or an APT coordinate, (also see Location).

Screen truth

A checkpoint's true position on the computer monitor as determined by observation.

Subpoint

The earth location directly under the satellite.

II. Historical Development

Works Prior to Larcomb

Before Larcomb's effort, several authors published works in registering geographical data to satellite images. Two predominate algorithms appear to abound in the literature, those that use pattern recognition techniques and those that use a combination of satellite position information with viewing geometry.

The pattern recognition technique requires that the image contains features that are recognizable to a person or machine (computer). This restricts registration to geographical areas that include land features not obscured by clouds. Seasonally changing features such as snow, ice and changing water levels (lakes, rivers, tidal flats, etc.), make pattern recognition techniques difficult to implement in some applications [1:202]. Larcomb compared and contrasted most of the works that used satellite position information along with viewing geometry [3:7-10]. The viewing geometry developed by the authors were of two major types. Some assumed a spherical earth model while others assumed an oblate spheroid model. Most techniques varied in their use of ground control points, points identifiable on the ground to establish the satellite's position [5:5-9; 7:1257-1260; 8:47-51]. Larcomb's method is

one of two methods that attempts to avoid completely the use of ground control points. By using a very accurate orbital model, Larcomb's algorithm appears to have the most promise for generating accurate satellite positions. This increased accuracy should result in better pixel location measurements.

Larcomb's Model [3]

Larcomb compiled data to support his registration algorithm from many sources. He used a NOAA-supplied user's guide, NOAA technical memorandums, and a Department of Commerce information note. He cites the work of several other authors who have developed related algorithms. Background material presented supports his work well. After discussing the problem of registration, Larcomb enumerates the fundamental steps of the algorithm.

Larcomb attempts to measure the geographical position of pixels by precise satellite position information and viewing geometry. By combining the NORAD SGP (Simplified General Perturbation) orbital model along with an oblate-spheroid earth model, Larcomb's algorithm should reduce most computation errors to near zero. The predominant source of errors should be errors in input data. These may include time, orbital parameters, satellite stability, and sensor performance. Registration of data can occur in one of two different ways. Larcomb defines direct referencing as the calculation of the geographical (geodetic) coordinates of a

pixel. He defines inverse referencing as finding which pixel in a set of data corresponds to a given geographic location. Larcomb developed algorithms for both methods [3:70-74].

Satellites in orbit follow nearly elliptical paths. Some of the registration algorithms proposed previously used circular orbits as a close approximation. The TIROS-N series satellites do remain in approximately circular orbits with the apogee/perigee height difference being less than 56 km. Other authors used an elliptical model for an even better calculation. While these models produce better results than the circular orbit models, they begin to worsen in their accuracy as time passes due to various orbital perturbations. Orbital perturbations are forces that affect a satellite's motion, making it deviate from an elliptical model. The effects of certain perturbations increase with time, resulting in growing errors (when using simpler orbital models) since the last update of the orbital parameters. Larcomb used a model that incorporated the strongest perturbations that affect satellites in low-earth orbit. These perturbations include the earth's nonspherical shape and atmospheric drag. If a model does not account for the effects of these forces, the predicted position of the satellite will begin to grow in error over time.

When conducting direct registration, satellite position calculations will be required for each pixel. Larcomb suggests that the satellite's position can be approximated

as a change from an initial position generated by the NORAD SGP model. He proposes that a circular model can be used to save computation time, while still maintaining sufficient accuracy [3:60].

Inverse registration creates the additional problem of having to determine the time that the satellite viewed the desired latitude and longitude. This is done using an iterative procedure. First, the computer calculates an initial time estimate for when a sensor scan line would have crossed the location of interest, assuming no rotation of the earth. Next, it updates this estimate by accounting for the earth's rotation and the orbit's precession. Then, it repeats this process until reaching the desired degree of precision [3:63-64].

The remainder of the registration process consists of resolving the viewing geometry. In a fashion similar to the problem of satellite position, various authors proposed different models of viewing geometry. Larcomb used the oblate-spheroid model. He proposed that this would result in improved accuracy, while running faster than spherical earth models.

After resolving the viewing geometry problem, coordinate transformations are the only remaining problems to solve in order to complete the process. This includes proper conversions between geocentric and geodetic latitudes, and conversions between APT coordinates and screen positions.

The results are a means to convert pixel coordinates into geographic coordinates and back again. Although Larcomb did not develop display algorithms, his registration method produces data that can be displayed in any perspective desired [3:65-69]. Larcomb enumerates two algorithms to accomplish registration. He lists one for direct registration and another for inverse registration. A summary of these algorithms follows:

Direct Registration

Step 0: Measure the time of the first pixel in the data set imaged, then compute satellite position and velocity for that time using the NORAD SGP model. Calculate the subpoint geocentric latitude, and the longitude and time of the ascending node.

Step 1: For each pixel, calculate its time and scan angle. Transform APT coordinates to HRPT coordinates if necessary. Calculate pixel scan angle and scan time.

For each pixel do:

Step 2: Compute satellite position and velocity using either the NORAD SGP or spherical orbit approximation.

Step 3: Compute or update scan direction, as required.

Step 4: Compute range from satellite to image point.

Step 5: Compute the earth position vector.

Step 6: Calculate geocentric latitude and longitude.

Step 7: Convert the geocentric latitude to geodetic latitude.

Inverse Registration

Step 0: Measure the time of the first pixel in data set imaged. Calculate the satellite position and velocity for that time.

For each earth location do:

Step 1: Convert geodetic latitude to geocentric latitude.

Step 2: Compute equator crossing time and longitude.

Steps 3-6: Estimate the time that the satellite viewed the pixel using an iterative method.

Step 7: Accuracy can be checked at this point. Geographic coordinates can be computed using the time estimated in Steps 3 through 6. The difference between the resulting location and the desired location can then be directly compared, and additional steps can be taken, if desired.

Step 8: Compute scan angle.

Step 9: Compute pixel coordinates.

Larcomb's registration algorithm can be treated as a measuring instrument. What is being measured is the geographical location of a pixel. As an instrument, its usefulness needs to be determined by some means of validation. There must be some correspondence between the value determined by the algorithm and the actual location of the pixel. Furthermore, any measuring instrument has limits to its accuracy and precision, the extent of which should be determined before the instrument can be used for careful measurement.

Validation and Sensitivity Analysis

Since the scope of much of this thesis is to develop a measure of validity for the Larcomb registration algorithm, an investigation into what a proper validation consists of will be examined. Dominowski defined validity as, "the extent to which a measure accurately represents a variable as conceptualized," or, "the extent to which a measure reflects the theoretical construct that a researcher has in mind" [2:42,262]. This extent can be quantified as a correlation between a measured value and some other value to which it relates.

Dominowski has suggested that reliability can be used as a more stringent measure of validity when the measured value is theoretically indistinguishable from the related value. Reliability refers to "the stability or consistency of the values that are obtained" [2:42]. Dominowski discussed three methods to measure reliability, each representing a more precise definition of it. Of these methods, internal consistency will prove to be a useful measure to the problem of registration reliability. The idea of internal consistency as discussed by Dominowski, when applied to the problem of registration accuracy, is that there should be a high degree of correlation between measurements when repeating a test several times [2:259].

Much of the focus of Dominowski's book is on research in psychology. Although at first sight it would appear that this would limit the applicability of the techniques that he suggests, this is not so. Psychological tests often consist of many small tests (questions), each of uncertain capability to make a reliable measurement. For example, no intelligence judgment (as in IQ tests) will be made based on a single question. In a similar manner, the ability of Larcomb's registration technique to determine a pixel's location depends on the accuracy of many aspects that are not in the direct control of the program. These aspects induce some doubt of the actual accuracy of his technique. By analyzing data regarding the accuracy of his technique, conclusions about its general reliability can be made.

Correlation between measured and accepted values provides a measure of validity for an instrument. Additional validity can result by determining an instrument's precision and accuracy. Mandel describes precision by describing imprecision. He states imprecision is, "the amount of scatter exhibited by the results obtained through repeated application of the process to that system" [4:103].

Mandel defines accuracy as, "the absence of bias" [4:105]. As a measure of accuracy he proposes the difference between the mean of a population of measurements and a reference value. This reference value may be either some real or true value, an assigned value, or some

hypothetical value that is equivalent [4:104]. For this thesis, the geographical coordinates of an identifiable point can be treated as an assigned value, while a measurement made in the image space (pixel coordinates) can be considered a hypothetical value.

III. Modifications to Larcomb's Algorithm

After the publication of his thesis, Larcomb identified several corrections and improvements. For readers who have previously obtained his thesis, an errata should be available. Improvements proposed by this author are described here. Some of these changes are intended to improve accuracy. Others are intended to increase the utility of the method by allowing for descending passes and southern hemisphere cases.

Orbital Mechanics

The NOAA polar-orbiting weather satellites are kept in nearly sun-synchronous orbits. This is done by placing the satellites into orbits with inclinations of 97.8 degrees. This placement should result in an orbital precession rate of 6.844774×10^4 degrees/minute as indicated by Larcomb [3:63]. While this is ideally correct, an improvement can be made to allow for orbits that differ in inclination. Since the SGP model calculates the orbital precession rate, a more accurate value can be used for nodal point and static longitude calculations.

Viewing Geometry

The accuracy of the sensor scan angle calculation is strongly dependent on knowing ψ , the earth's radius (see Appendix G), and the satellite's orbital radius. The angle ψ is the earth center angle between the satellite's subpoint S , and earth location E . The greatest sensitivity to errors in radii occurs where the scan angle is at its extremes, near the edges of the image (swath). The sensitivity to errors in either radius is a function of scan angle. At the worst case, a 1-km error in radius will result in a location error of roughly 2 km; therefore an accurate satellite orbital radius is needed for an accurate scan angle result. A NOAA satellite orbit during a typical pass may change in orbital radius by 10 km. This will result in radius deviations of 5 km from the radius at the image midpoint. If this is not considered, the resulting location error can be roughly 10 km or 3 pixels.

This error would be a significant source of error during inverse referencing. Direct referencing will normally not be affected since it can use an accurate radius from the SGP model. Larcomb used a "locally circular model" to accomplish inverse referencing. Even though the circular model is used to determine the location of the subpoint, the actual satellite orbital radius or some approximation to it could be used in the scan angle calculation. Using the actual orbital radius would require multiple calls to the orbital model. This is a time-consuming process when used

in an iterative procedure, so an alternative method was developed. A nonlinear, quadratic regression is used to calculate a polynomial approximation. Three points along the satellite's path are found to be sufficient to model accurately the satellite's orbital radius as a function of time. The beginning, middle and end portions of the pass are chosen to avoid extrapolation. The resulting expression returns the satellite's orbital radius as a function of time. This technique is only slightly more computationally intensive than using a constant, as in the locally circular model, yet much faster than repeated calls to the NORAD SGP orbital model. Tests of this technique shows that the satellite's orbital radii are within 0.001 percent of that computed by the orbital model, eliminating this source of error without significantly increasing computation time.

Direct Referencing

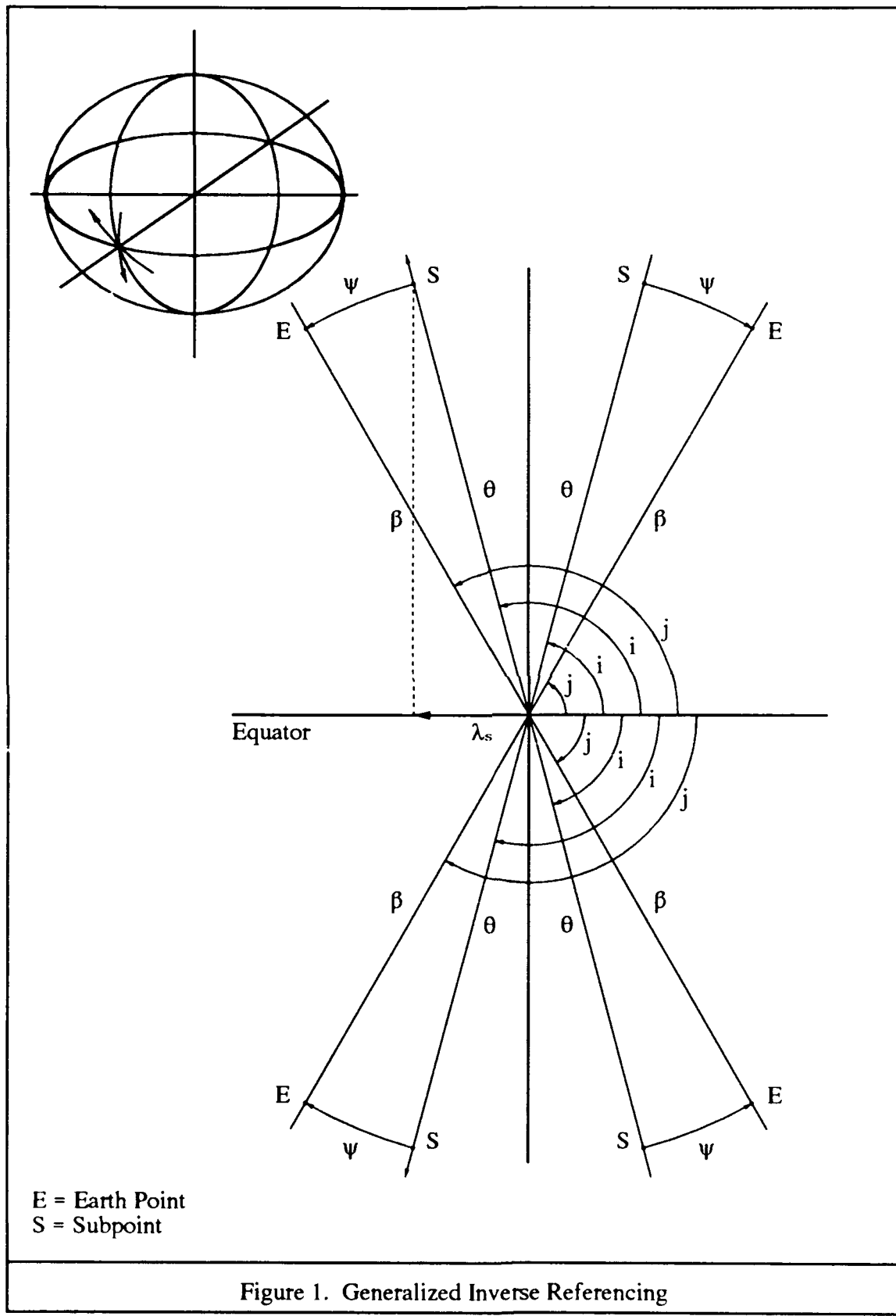
The direct referencing algorithm is a vector solution to the registration problem. Central to the vector problem is the determination of the satellite's position and velocity. Larcomb proposed that either an elliptical (SGP) or a circular orbital model may be used to calculate these values [3:60]. If a circular model is used it will be subject to the same type of errors discussed in the last section, but it requires less computation. A test of the two techniques showed that the elliptical model required three times as long to run. It also should be noted,

however, that direct referencing is normal not used repeatedly during gridding or outlining. Therefore speed may not be nearly as important as accuracy. For the tests in this paper the elliptical model was used.

Inverse Referencing

In his development of an inverse referencing algorithm, Larcomb modeled an ascending pass (satellite moving from south to north) where the imaged area lay in the northern hemisphere. The algorithm requires the identification of the equatorial crossing point, in particular the ascending node. This model can be generalized to provide worldwide coverage with some modifications. Two areas of improvement are proposed. The first is a means to calculate the equator crossing point (nodal point) regardless of pass direction or hemisphere. The second is a means to calculate the scan time regardless of pass direction or hemisphere.

Nodal point calculation begins by picking any satellite subpoint as a starting place, see Figure 1. The midpoint of the pass or image serves best when considering the effects of short-term periodic perturbations.



By treating θ , the earth-centered angle between the nodal point and the midpoint, and θ' as signed quantities, the nearest nodal point can be calculated. This point may be either an ascending or a descending node. The angle θ is defined as

$$\sin \theta_S = \sin \Phi_S / \sin i \quad (1)$$

where

Φ_S = latitude of the subpoint
 i = satellite's inclination

and the of change of θ is

$$\theta' = \mu / r^3 \quad (2)$$

where

μ = earth's gravitational constant
 r = satellite's orbital radius

The sign of θ' must be set to equal the sign of v_z , which is the satellite's component of velocity in the polar direction. This value is obtained from the SGP model. In the development pictured in Figure 1, θ is positive for midpoints in the northern hemisphere, and negative for those in the southern hemisphere. Similarly, θ' is positive for ascending passes, and negative for descending pass. The nodal crossing time is calculated as before as

$$t_N = t_S - \theta_S / \theta' \quad (3)$$

The results will be after the midpoint time for those passes approaching the equator. This may be either an ascending pass in the southern hemisphere or a descending pass in the northern hemisphere. The other cases correspond to nodal

crossing times occurring before the midpoint time.

The subpoint static longitude is given by

$$\cos \lambda_S = \cos \theta_S / \cos \phi_S \quad (4)$$

The sign of the subpoint static longitude, the angular difference between the subpoint longitude and the nodal crossing point, is defined as negative for passes with midpoints to the west of the nodal point. Since the law of cosines is an even function, it will always result in positive angles. Therefore the sign of λ_S must be changed when the nodal crossing time is before the midpoint time. After calculating the above signed quantities, the nodal point longitude can then be calculated as before as

$$\lambda_+ = \lambda_S + \lambda'_S + (t_S - t_N)(\omega - \Omega') \quad (5)$$

where

$$\begin{aligned} \omega &= \text{earth rotation rate (0.2506845 degrees/minute)} \\ \Omega' &= \text{orbital precession rate} \end{aligned}$$

The calculation of the time for the imaged location must be modified to consider the various possibilities of pass direction and hemisphere. By developing sign conventions, and by making some adjustments to angles, worldwide inverse referencing can be accomplished (see Figure 1). Included in this figure are the four possible cases of pass direction and hemispheric location. Differences between this development and that proposed by Larcomb are noted here.

The angle j is the angle between the equator and the great circle through the nodal point and the earth location. It is now a signed quantity, positive for imaged locations in the northern hemisphere:

$$\sin j = \sin \Phi_E / \sin \beta \quad (6)$$

The angle i is no longer the inclination of the orbit as it is for the northern-hemisphere, ascending-pass case. It is defined as the angle between the satellite ground track and the equator, and it is positive when the imaged location is in the northern hemisphere. This is summarized as follows:

Hemisphere	Pass Direction	i equals
Northern	Descending	Inclination
Northern	Ascending	π - Inclination
Southern	Ascending	Inclination - π
Southern	Descending	- π - Inclination

The angle ψ is the earth center angle between subpoint s , and earth location E . Care must be taken to ensure the proper sign is applied so the scan angle calculation will be correct:

$$\sin \psi = \sin(j-i) \sin \beta \quad (7)$$

The angle θ is the satellite orbit angle measured from the nodal point. It is now a signed quantity, positive for satellite subpoints that are after equatorial crossing. This convention is needed in the scan time calculation. These changes complete those necessary to generalize the inverse referencing algorithm.

Larcomb's inverse referencing procedure uses an iterative approach to estimate the viewing time. As he

suggests, any time corresponding to a point near the imaged area will work as a starting time. In practice, the inverse referencing procedure will usually be used to grid or outline an image. Because of this, it will be called hundreds or thousands of times per image. Normally, the points will be referenced in some kind of order, that is, geographically close (or adjacent) points will be processed sequentially. By using the scan time from the last solution as the starting time for the next iteration, convergence will normally occur much faster. Tests show that when the time of the first line received was used as a starting time, convergence occurred in about 4 iterations. By using the previous solution as the starting point, convergence normally occurred on the first iteration. Processing time is less than half of that previously required. The above test was done using locations in a sequence near each other, like those that occur during gridding.

IV. Methodology

The validation of an algorithm involves testing of the algorithm under both simulated and actual conditions.

Several tests are used to establish the various aspects of validation discussed by Mandel and Dominowski. These are broken down into two categories: verification and validation. To aid in testing of the algorithm, modular program design was used.

Modular Program Design

Modular program design is the concept of breaking a program down into parts. Each part of the program is responsible for a particular aspect of the task to be accomplished. This type of program architecture results in several benefits useful for validation and program development. See Figure 2.

A collection of routines (procedures and functions) can be created and easily used in different programs. Once these routines are written, they can be used with little or no knowledge of how they work. Modularization allows program developers to write programs that use registration without worrying about the details of how to do the registration. It also ensures that the procedures perform identically in different programs. For example, the results

Data Flow Diagram

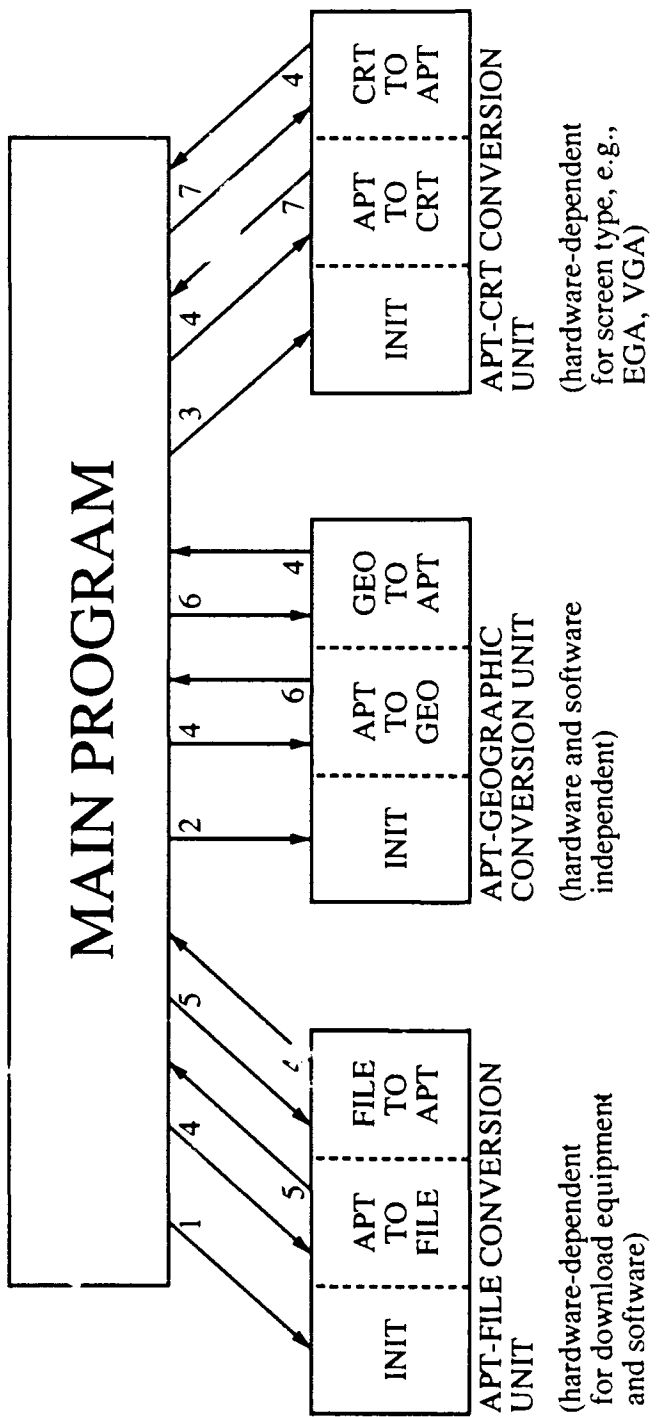


Figure 2. Data Flow

obtained in test programs will also be obtained in application programs because the module can be used in both without modification. Finally, this approach results in a validated algorithm and in tested and validated code at the same time.

The source code can be secured. That is, since a program module can be compiled ahead of time, the source code does not have to be released for the module to be useful. This prevents unwittingly modifying the code, which may keep it from working properly.

Modules that are written to be machine-independent can be used in programs on any computer. Only the machine-dependent modules will have to be modified to port the code to other computers.

Pascal was chosen for this project for its speed, modularization, and its being widely accepted as a high-level language on personal computers. In Pascal a module is called a unit. In order to validate the registration algorithm several units were written. Both, machine-dependent and machine-independent units were required. These are described in greater detail in the Appendix. Note that the unit that does registration is completely machine-independent.

Verification

Verification is done to establishing that the computer program executes as intended. This was accomplished using two techniques: separate testing of the various components of the program and internal consistency checks for inverse functions.

Component testing consists of simply checking that all intermediate calculations are being done correctly. Particular consideration must be given to special cases such as calculations involving the northern and southern hemisphere, and the polar and equatorial zones.

A powerful test for verification results from the fact that direct and inverse referencing are reciprocal functions. By doing a direct reference on a given position and then doing an inverse reference on the resulting location, one should arrive back at the starting point. A special program was written to accomplish this test. It operates like this: First, the referencing unit is initialized for a satellite pass. The time and date do not have to correspond to a real image although it should be realistic (reasonably close to the element epoch time). Special times can be used to position the satellite over a pole, the equator, or any place desired for the test. Next, direct referencing for a spread of positions in APT coordinates is then accomplished, followed by inverse referencing for the resulting locations. The end positions

are then compared with the starting positions. Finally, differences can be noted and displayed graphically.

Validation

To establish validation, a level of correspondence between calculated and "ground true location" values were established. Both direct and inverse measurements were made on many observations and statistically analyzed. To make the measurements, a special program subroutine was written.

In preparation for testing the registration algorithms, a collection of checkpoints was created. This thesis will treat these points as known locations in the same way that other registration techniques use ground control points as known locations. These checkpoints were selected based on several criteria: land/water contrast, limited seasonal variation, uniqueness, and identifiable pixels.

Land-to-water contrast is the most identifiable geographic feature in NOAA satellite images. In order for ground checkpoints to be useful they have to be visible. Every checkpoint used for validation featured land-to-water contrast.

While some water-related features undergo seasonal variation (such as intermittent lakes and streams), others do not. In order to minimize seasonal changes, lakes and reservoirs with tributaries were chosen. Reservoirs are considered especially desirable because of their ability to control the water level thus stabilizing the shoreline. Dam

sites were chosen for their steep sides and deep water. Swamps and marshes were completely avoided.

Geographical features that were somehow unique to the local area reduce the chance of being visually confused. Lakes were used only where they were well separated from each other. Likewise, bays were used in lakes and along coastlines only where there were relatively few bays in the area. Rough or irregular coastlines were avoided since their features are too small and too close together.

The selected checkpoints had to be identifiable to a single pixel in the image. Features nearly the size of a pixel, 3 to 4 km, fit this requirement best. Those smaller than 3 km may not resolve well, while those that are larger left ambiguity on the exact location of the target in the image. Under some conditions, even a perfect checkpoint would appear to straddle two or more pixels making it impossible to identify its exact pixel location.

In addition to the above criteria, a uniformed distribution within reception range is desired. The final set of checkpoints are illustrated in Figure 3.

The checkpoint measurements were taken from Defense Mapping Agency Jet Navigation Charts. These maps are normally used for high-altitude jet navigation by military pilots. Three charts, JNC-43, JNC-44, and JNC-45 provide complete coverage of the United States, Southern Canada, and Northern Mexico. Since these charts are used for

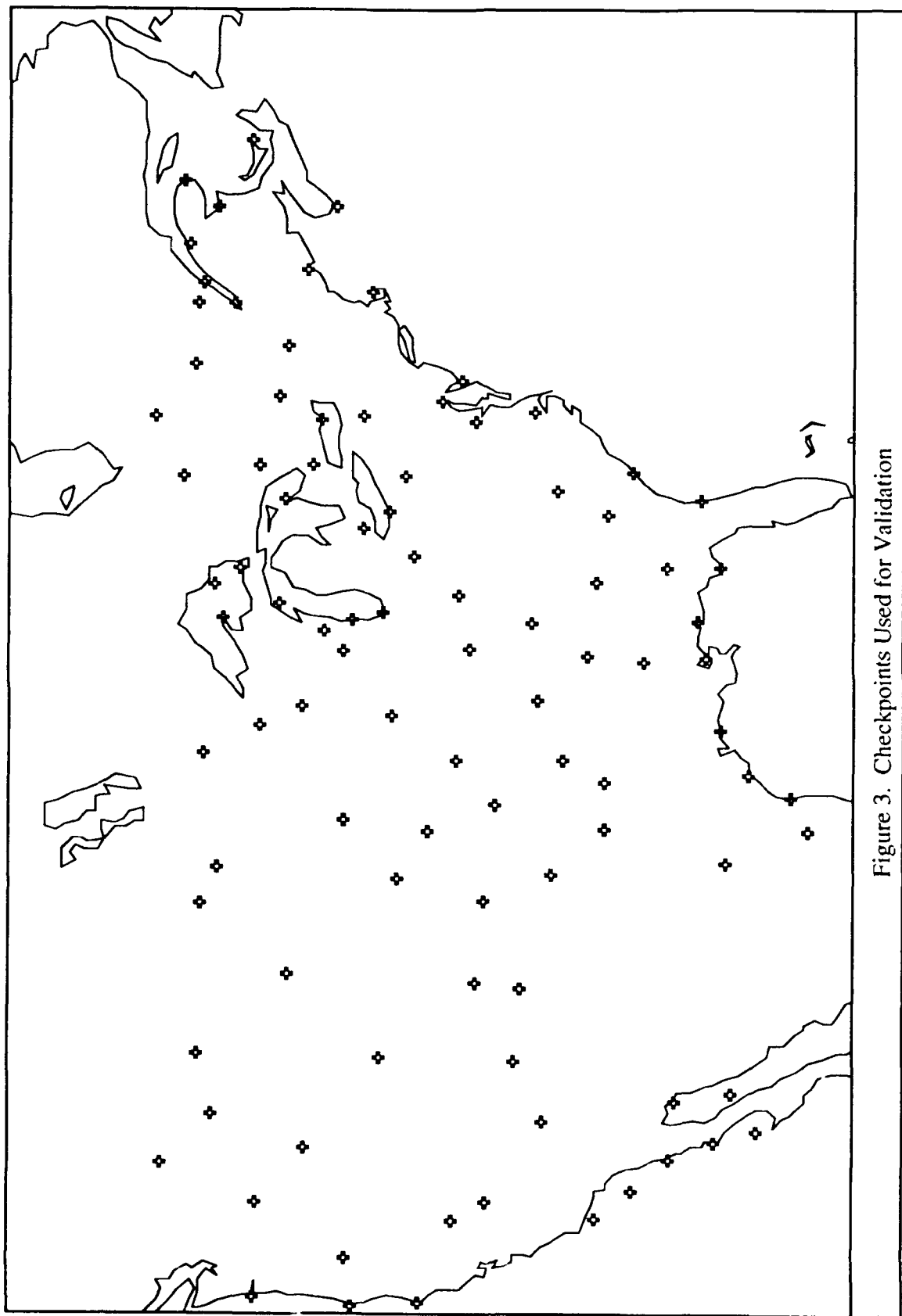


Figure 3. Checkpoints Used for Validation

navigation, the position and shape of geographical features are plotted with a high degree of accuracy. They were compiled in 1971 and were revised in 1988, 1986, and 1985, respectively. The scale of the charts, 1:2,000,000, corresponded well with the resolution of APT data. Objects that were barely discernible in the satellite images were only slightly more discernible on the map. This was a desirable feature that aided in the identification of checkpoints.

The process of measuring errors was done with the help of a special subroutine in the main program. This subroutine sequentially prompts the researcher to identify each checkpoint's screen position. It then builds a computer data file containing data regarding the performance of the referencing procedures. This data can then be statistically analyzed. The process can be broken down into the following steps:

1. Read the checkpoint information from the checkpoint data file. This information includes the checkpoint's name, a description of the checkpoint that can be used to identify it visually, and its ground truth location.
2. Execute an inverse reference procedure on the ground truth location to test to see if the location is displayed on the current satellite image. This makes the assumption that the inverse referencing procedure is accurate to a few pixels, which was confirmed by preliminary tests. If the point is not on the screen, go to the next point, or else save the calculated screen position and continue.

3. Magnify the area of the screen that is calculated to contain the checkpoint and place a cursor over its expected position.
4. The researcher then moves the cursor to where he identifies the screen truth position. This point is then stored.
5. Execute a direct reference procedure on the screen truth position. The resulting calculated ground location is then stored.
6. Write the following information out to a disk file: ground truth location, calculated ground location, screen truth position, calculated screen position, satellite number, image date, image time, element epoch time, and image file name.
7. Go to Step 1 and repeat until all of the checkpoints have been measured.
8. Repeat for each satellite image to be tested.

The data file is then processed to calculate errors.

Along-track, cross-track, great-circle distances and directions are added to it. The resulting data file contains a data base of observations that can be analyzed in many ways. Analysis can be accomplished on all the data simultaneously or on selected subsets. There is sufficient data in each record (observation) to test both the direct and inverse referencing procedures.

This information was analyzed using several tools. A statistical analysis program and a spreadsheet were used to calculate accuracy, and a custom graphics program was used to aid in sensitivity analysis.

Measures of Performance

Location Accuracy is the difference between the results of direct referencing and the checkpoint's ground truth location. Position Accuracy is the difference between the results of inverse referencing and the checkpoint's screen truth position. Ideally, both of these quantities should be small and without bias. Correlations between errors and scan angle, latitude, scan line, or other quantities may indicate deficiencies in the models. Once identified, improvements to the models can be made.

Sensitivity Analysis

The sensitivity analysis is intended to develop a feel for how errors in the input data affect registration accuracy. Sources of errors include: the orbital element set, the download equipment, and the satellite's operation. This thesis will limit its examination to errors in inclination, right ascension of the ascending node, eccentricity, mean motion, image time, and attitude control.

The effects of some errors can vary depending on the satellite's position at the time of image receipt. For example, an error in the reported inclination will have a greater effect near the poles than it would at the equator. For these errors, only a typical case (mid-latitude, North America) will be considered.

Vector fields will be used to display quantitatively the magnitude and direction of registration errors. These

fields are generated by making two sets of registrations over a range of APT coordinates. On a vector field display, a vertical line down the center of each chart depicts the satellite's ground path. The vertical lines at the left and right edges depict the limits of the ground swath. The small squares represent the true locations or positions. The line extending from the center of the square points in the direction of the error, and its end shows where the position would be plotted with the error. For examples, see Figures 8 through 16 in the next chapter. Further explanation of these figures will be discussed there.

The first set of registrations is assumed to be perfect, it will be used as an experimental control. The second set of registrations will be made with modified values in the orbital element set or satellite attitude to simulate errors. The difference between the two sets of registrations represents the inaccuracy that will result from errors in these sources. These sets of registrations are done on a group of points in the form of a rectangular array in the image space. These points are direct referenced to calculate geographical locations. Next, these locations are inverse referenced to generate a new set of APT coordinates. A special test program, which uses the referencing unit, was written to do this. In addition, it plots the difference between the control data and the modified data in the form of a vector field.

V. Results and Discussion

Verification

Inspection of the Pascal code after the modifications were made revealed a well-structured, object-oriented code that closely parallels the registration algorithm. The code is expressive, using statements, constants, and variables analogous to those used by both Larcomb and this author in their theses.

Both of the referencing procedures transform coordinates between geographic coordinates (geodetic latitude/longitude) and APT coordinates (scan line/pixel number). Since APT coordinates are a function only of the NOAA weather satellite's operation, these procedures should work with any image capture system. In order to relate the computer monitor's (CRT) coordinates or a file position to APT coordinates, transformation functions are needed. In general, the transformation function is a function of APT data rate, digitizer sample rate, and the data-reduction ratio. APT data rate is the rate that the satellite transmits data. The digitizer sample rate is the rate that the analog APT signal is converted into pixels by the image capture equipment. And the data-reduction ratio is the ratio of bytes saved to those received, which is used to keep image files from becoming too large. These functions

were written for the test programs by the author (see Appendix B).

The verification test program was run on theoretical data for each hemisphere, at the poles, and over the equator. In each case, the registration was internally self-consistent. Starting with APT coordinates, direct referencing followed by indirect referencing was accomplished for 400 positions per frame. The maximum difference between the start coordinates and final coordinates occurred in the corners of the frame. The maximum error observed was 0.15 APT pixels. The average deviation was 0.03 pixels. Therefore, the procedures appear to behave as true reciprocal functions of each other.

As noted in Chapter III, direct referencing is based on a straightforward vector model while inverse referencing is based on an iterative, spherical trigonometric solution. Since the direct referencing model is fundamentally independent from the inverse referencing model, their near agreement as reciprocal functions adds validity to the algorithms. That is, the algorithms are consistent with each other even though the computations are quite different. This consistency will form the basis for conducting the sensitivity analysis.

It should be noted here that the initial outcome of this test resulted in many modifications to the algorithm and code. Typographical errors in the referencing unit were quickly spotted as a result of this technique. This

verification method also identified the inherent inaccuracy of the constant altitude model of inverse referencing.

Validation

The validation was accomplished using 78 images from the NOAA 11 spacecraft. These images were gathered during a period of 61 days, from 6 June to 5 August 1990. The decision to use only one spacecraft was an attempt to limit the number of variables in the test. During each day, a pass over the eastern United States was captured. On 17 days, a pass over the central United States was also captured. All passes were ascending. During this period NOAA 11 developed an attitude control problem [6:5]. This information was not known to the author until after the images for the experiment were collected. The attitude control problem resulted in temporary satellite yaw deviations of up to one degree. These deviations will result in registration problems (see Figure 11). The problem will be most pronounced near the edges of the image. It is uncertain exactly which images were affected. Three images appeared to have a significant registration problem due to yaw. Small yaw deviations may have caused minor problems on some images that can only be detected in a statistical sense. Additional effects of attitude control problems will be discussed in greater detail later in this chapter.

The true screen position of a checkpoint had to be determined subjectively by the researcher. It was a goal to

identify this position to the nearest pixel. Only observations that the researcher had high confidence in were considered. Clouds, fog, and sun glint occasionally prevented positive visual identification of checkpoints. Out of potentially 2000 samples, 1469 were recorded for analysis. This works out to about 19 samples per image. The average geographical position of a recorded checkpoint was at 40 degrees north, 86.5 degrees west. This is near Chicago, Illinois. The average checkpoint appeared at CRT coordinate (355,240), which was close to the center of the screen. On the hardware used, this translates to an APT pixel position of 475, which is 21 APT pixels to the right (east) of nadir. The points were uniformly distributed over the screen area except for the lower-right corner where they were less dense. The lesser density in this area was caused by the presence of the Atlantic Ocean in many of the images.

Figure 4 is an image of the eastern United States before registration. The same image, overlayed with a map outline is depicted in Figure 5. This accuracy is typical of that obtained during the test. As noted in Chapter IV, individual points were used for testing. The map outline was used here for clarity.

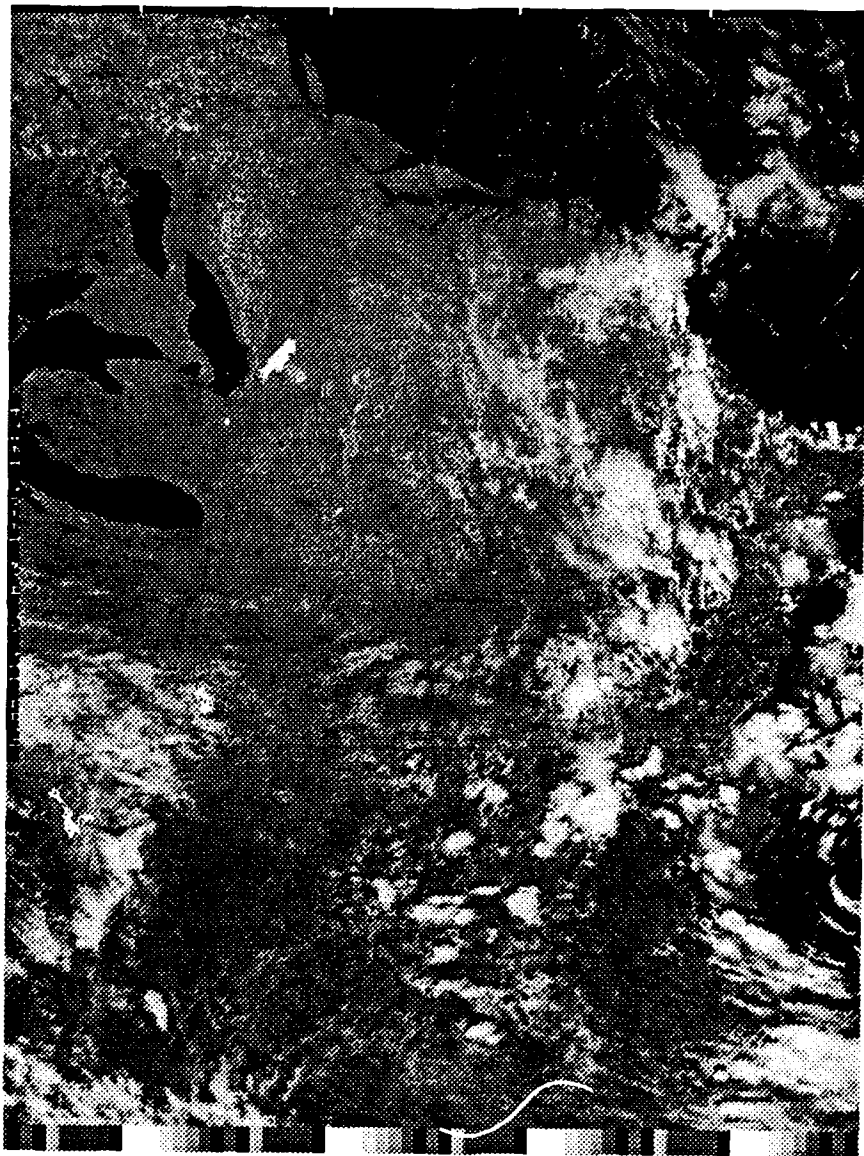


Figure 4. Image of Eastern United States

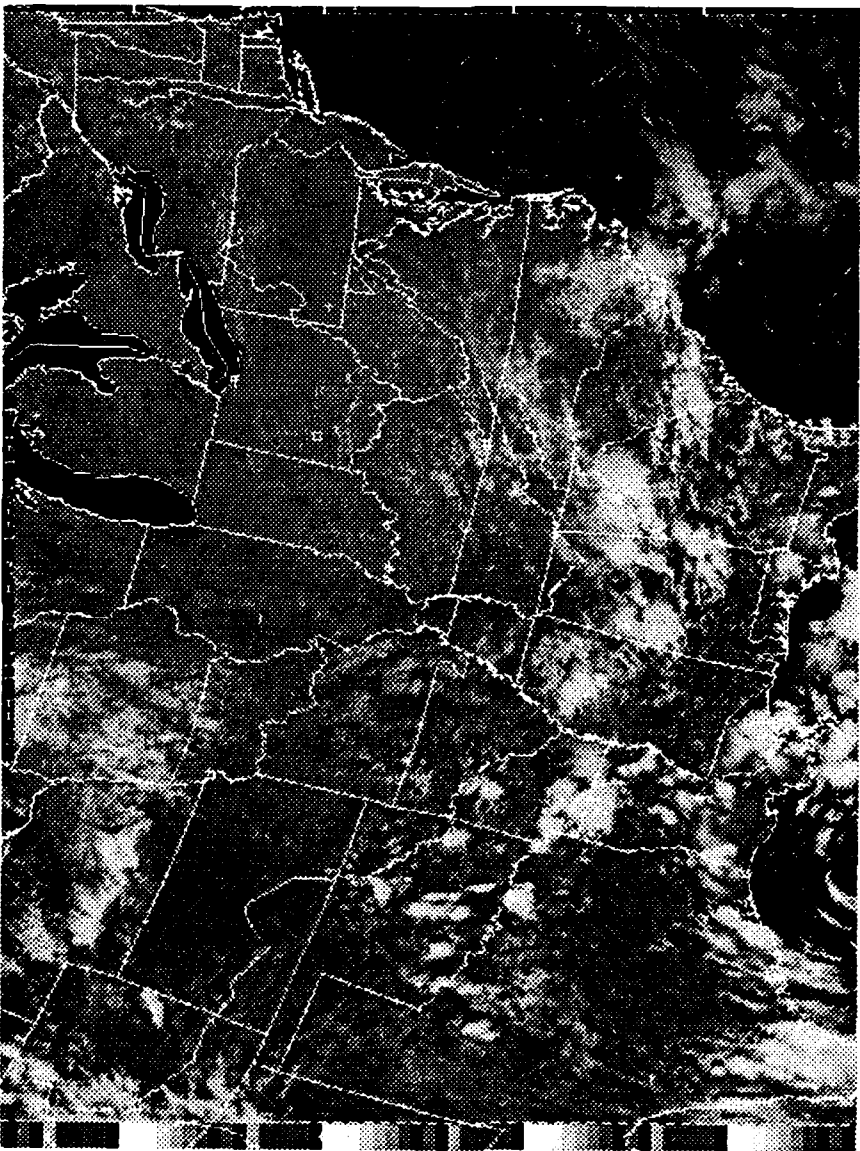


Figure 5. Registered Image of Eastern United States

Tables 1 through 3 list summary statistics for the group. The average location accuracy for the direct referencing procedure was 5.3 km, with 75 percent of all observations less than 6.8 km. The average position accuracy for the inverse referencing procedure was 1.3 CRT pixels, with 75 percent of all observations less than 2.0 pixels.

Errors in the screen's vertical direction can be treated as along-track errors while those in the horizontal direction can be treated as cross-track errors. By converting the pixel distances into equivalent angular distances, the outcome of the inverse referencing statistics can be compared to those obtained from the direct reference procedure. Using the relationships that

1 CRT line	= -1 APT line*
1 APT line	= 3.27 km (along-track)
1 km	= 1.57×10^{-4} radians of latitude
1 CRT pixel	= 1.3 APT pixel*
1 APT pixel	= 3.5 km (cross-track)
1 km	= 2.22×10^{-4} radians of longitude at 40 degrees of latitude

* this is display hardware specific

and beginning with the average cross-track and along-track errors (see Table 2), it can be shown that

$$-0.884 \text{ CRT pixels} = -1.15 \text{ APT pixels} = -4.0 \text{ km} \\ = -0.0009 \text{ radian longitude} \quad (8)$$

and

$$0.0647 \text{ CRT lines} = -0.0647 \text{ APT lines} = -0.21 \text{ km} \\ = -0.00004 \text{ radian latitude} \quad (9)$$

TABLE 1

Direct Referencing Statistics (radians)

Variable:	Ground Truth		Direct Referenced		Error			
	Lat	Lon	Lat	Lon	Lat	Lon	Dir (deg)	Dist (km)
Average	0.6942	-1.5362	0.6943	-1.5354	0.0001	0.0008	115.5920	5.2798
Median	0.6993	-1.5309	0.7000	-1.5288	0.0001	0.0006	88.7181	4.5174
Mode	0.6347	-1.5368	0.6745	-1.5590	0.0003	0.0005	88.5612	4.6531
Geometric mean	0.6883	0.6884		284.8960		85.7858	4.2235	
Std. deviation	0.0889	0.1989	0.0888	0.1991	0.0005	0.0008	88.9917	3.4999
Std. error	0.0023	0.0052	0.0023	0.0052	0.0000	0.0000	2.3219	0.0913
Minimum	0.4637	-2.1738	0.4652	-2.1727	-0.0015	-0.0015	0.3151	0.2084
Maximum	0.8689	-1.0818	0.8691	-1.0787	0.0036	0.0043	359.9680	23.0529
Range	0.4052	1.0920	0.4040	1.0940	0.0051	0.0058	359.6530	22.8445
Lower quartile	0.6286	-1.6645	0.6292	-1.6641	-0.0002	0.0002	58.9338	2.7748
Upper quartile	0.7645	-1.3980	0.7650	-1.3966	0.0004	0.0012	132.8420	6.8027
Inter. range	0.1358	0.2665	0.1358	0.2675	0.0006	0.0010	73.9080	4.0279
Skewness	-0.2495	-0.5566	-0.2500	-0.5519	0.7228	0.9221	1.4225	1.3489
Std. skewness	-3.9045	-8.7097	-3.9126	-8.6350	11.3094	14.4287	22.2583	21.1065
Kurtosis	-0.7714	0.4574	-0.7706	0.4511	4.6038	1.3322	1.1356	2.1328
Std. kurtosis	-6.0354	3.5788	-6.0286	3.5293	36.0179	10.4223	8.8843	16.6864

TABLE 2

Inverse Referencing Statistics (screen pixels)

Variable:	Screen Truth		Inverse Referenced		Error			
	X	Y	X	Y	Delta X	Delta Y	Dir (deg)	Dist (km)
Average	354.8740	239.5850	353.9900	239.6500	-0.8843	0.0647	167.6700	1.3070
Median	367.0000	216.0000	367.0000	216.0000	-1.0000	0.0000	243.4350	1.0000
Mode	371.0000	245.0000	127.0000	109.0000	-1.0000	0.0000	270.0000	1.0000
Geometric mean	176.8160		283.3530	176.9130				
Std. deviation	187.8320	149.9050	187.6580	149.9400	0.9354	0.9194	130.2730	0.8930
Std. error	4.9007	3.9112	4.8962	3.9121	0.0244	0.0240	3.3989	0.0233
Minimum	18.0000	3.0000	16.0000	4.0000	-4.0000	-3.0000	-75.9638	0.0000
Maximum	713.0000	537.0000	711.0000	538.0000	2.0000	6.0000	270.0000	6.3246
Range	695.0000	534.0000	695.0000	534.0000	6.0000	9.0000	345.9640	6.3246
Lower quartile	191.0000	115.0000	191.0000	115.0000	-1.0000	0.0000	0.0000	1.0000
Upper quartile	507.0000	359.0000	507.0000	359.0000	0.0000	1.0000	270.0000	2.0000
Inter. range	316.0000	244.0000	316.0000	244.0000	1.0000	1.0000	270.0000	1.0000
Skewness	-0.0264	0.3089	-0.0349	0.3090	-0.6620	0.5300	-0.8201	0.8804
Std. skewness	-0.4130	4.8335	-0.5465	4.8342	-10.3582	8.2937	-12.8316	13.7765
Kurtosis	-1.1089	-1.0488	-1.1119	-1.0497	0.3897	3.7177	-1.1161	2.0229
Std. kurtosis	-8.6758	-8.2050	-8.6990	-8.2124	3.0491	29.0860	-8.7320	15.8265

TABLE 3
Epoch and Minute Mark Statistics (minutes)

Variable:	Epoch Times			
	Image	Elements	Difference	Nudge Time
Average	90189.1000	90188.2000	-0.8908	-12.3281
Median	90187.8000	90185.3000	-0.8544	-12.0000
Mode	90179.8000	90206.2000	0.4215	-12.0000
Geometric mean	90189.1000	90188.2000		
Std. deviation	17.4859	17.4944	1.3655	0.5424
Std. error	0.4562	0.4564	0.0356	0.0142
Minimum	90157.8000	90157.4000	-4.3985	-13.0000
Maximum	90217.9000	90214.4000	2.5482	-11.0000
Range	60.0400	56.9900	6.9467	2.0000
Lower quartile	90175.8000	90176.0000	-1.6349	-13.0000
Upper quartile	90206.8000	90206.2000	0.2798	-12.0000
Inter. range	30.9700	30.2700	1.9147	1.0000
Skewness	-0.0445	-0.0606	-0.0418	-0.0215
Std. skewness	-0.6963	-0.9480	-0.6545	-0.3359
Kurtosis	-1.1546	-1.1296	-0.3250	-0.7343
Std. kurtosis	-9.0334	-8.8372	-2.5427	-5.7452

These values are close to the 0.0008 radians of longitude and the 0.0001 radians of latitude values obtained by the direct referencing procedure (see Table 1). The minus signs obtained here indicates that their errors are in the opposite directions.

Another comparison of a similar nature can be made by comparing the distance and direction of the errors. On the hardware/software combination used, APT pixels can be compared to geographical coordinates. Using the approximate that

$$1.25 \text{ APT combined pixels} \approx \text{one CRT pixel*} \quad (10)$$

$$1 \text{ APT pixel} \approx 3.4 \text{ km}$$

* this is display hardware specific

and beginning with the average inverse error distance it can be shown that

$$\begin{aligned} 1.3 \text{ CRT pixels} &\approx 1.6 \text{ combined APT pixels} \\ &\approx 5.5 \text{ km} \end{aligned} \quad (11)$$

By these relationships, the average CRT error of 1.3 pixels corresponds to 1.6 APT pixels or 5.5 km. This compares well to the average error from the direct referencing procedure of 5.3 km. Finally, note that the median headings are roughly reciprocal headings.

As the above discussion suggests, the performance of the direct referencing procedure appears to be approximately equal to, but in the opposite direction of, the performance of the inverse referencing procedure. The rest of this analysis will be limited to inverse referencing.

Application to the direct referencing procedure can then be deduced for the remainder of this thesis.

The average vertical or along-track error was 0.06 scan lines. This statistic may be somewhat unreliable because of difficulty in establishing the precise time of reception. As stated in Chapter I, the minute marks in the image now can be used to establish the precise time of receipt, but this was not the case before 8 August 1990. During the period that the images were received, the minute marks did not correspond to Coordinated Universal Time (UTC). An attempt was made to determine the difference between the marks and UTC by registering a sample of images. The number

of scan lines of vertical error was used to determine the number of half-seconds the minute marker differed from UTC. A regression analysis was done and the results applied to the images (see Figure 6). As noted in Chapter I, the time of image receipt is based on the position of the minute marks in the image. Therefore the time that was originally calculated based on the minute mark position is corrected by the apparent amount of minute mark drift. From the regression analysis, it appeared that the minute mark drifted at a linear rate of 13.3 milliseconds/day. This rate correlates well to the 12 to 17 milliseconds/day satellite master clock drift rate for this period. Although no definite connection between the two drift rates could be confirmed, the tie seems reasonable. By applying the linear drift correction to the images it was hoped that problems that could cause vertical registration errors in the images would still be spotted. In any case, the distribution of vertical errors is still reliable although the average reported vertical error may have been zeroed out by this process.

Minute Mark Deviation from UTC

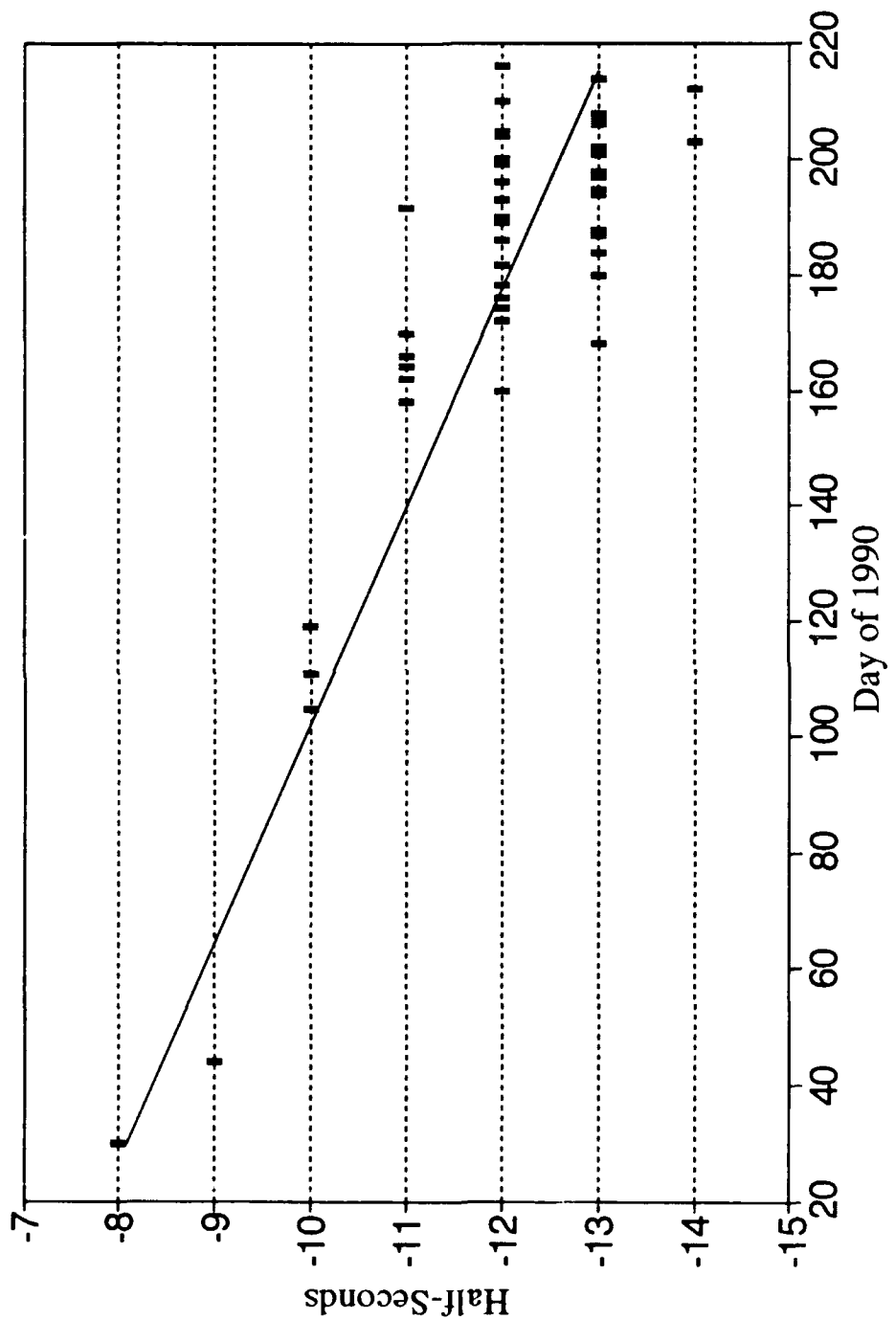


Figure 6. Regression Analysis of Minute Mark Drift

The average horizontal or cross-track error was -0.88 CRT pixels or 1.2 APT pixels. This accounted for most of the registration error observed. Usually, this error was greatest on the eastern side of the image. This tendency was very evident during testing. Only 36 observations showed a positive cross-track error, while 922 observations showed a negative error. The remaining 511 observations showed no cross-track error. No particular cause could be identified as of this writing. A possible explanation regarding satellite attitude control is discussed below.

The general impression from the testing was that registration errors were a function of their position on the screen. This dependence is most likely caused by the point's relative position in the satellite's swath. Multiple linear regression was used to model cross-track errors (CTE) and along-track errors (ATE) as functions of their CRT coordinates. Tables 4 and 5 summarize the results of the regression.

TABLE 4

Regression Analysis for Observed Cross-Track Errors

Variable	Coefficient	Std. Error	t-Value	F-ratio
Constant	-1.72189	0.05499	-31.313	
X_3	0.00603	0.00025	24.486	599.57
X_2	-1.58×10^{-8}	5.13×10^{-10}	-30.930	446.31
r^2	0.4156			

TABLE 5

Regression Analysis for Observed Along-Track Errors

Variable	Coefficient	Std. Error	t-value	F-ratio
Constant	0.41906	0.05023	8.3429	
X_2	-0.00100	0.00013	-7.9822	63.71
r^2	0.0410			

The resulting expressions for errors are:

$$CTE = -1.72189 + 0.00603 * X - 1.58 \times 10^{-8} * X^3 \quad (12)$$

$$ATE = 0.41906 - 0.00100 * X \quad (13)$$

The coefficient of multiple determination (r^2) value of the cross-track error regression indicates only modest support for Equation 12. The low r^2 for the along-track error suggests that only the trend information is useful, predicted values will be very uncertain. Visual inspection of scatter-graph data reveals that many observations are 1 or 2 pixels from the predicted value. The regression analysis strongly suggests that errors are not a function of the Y coordinate. The other terms are determined to be significant by a confidence level of 99 percent.

These functions were combined to produce a vector field of registration errors (see Figure 7). Confidence in the portrayal of vertical errors must be tempered by the low r^2 for along-track errors. The end product resembles the general trend of errors that were observed.

The above equations could be used to improve overall registration by applying corrections to the results of the algorithm. While this will improve the results of the

images used in this test, it is uncertain if it will work in general. The overall errors observed may be specific to the NOAA 11 spacecraft, or to some other cause not applicable universally. Before attempting to improve registration this way, more data will have to be collected in order to ensure that these are general errors applicable to all cases.

These errors are likely to be the consequences of one or more factors. One factor known to be included, is the attitude control yaw problem occasionally experienced by the satellite. Another factor, suggested by sensitivity analysis, is a possible roll problem as well (see Figure 10). A comparison between Figure 7 and Figures 10 and 11 suggests that Figure 7 includes characteristics of both. This is only one possible explanation. Other factors require scrutiny. For example, satellite sensor operation could explain the cross-track error. The sensor in the NOAA 11 spacecraft might not be operating as modeled in the registration unit. Or, the problem might lie in the algorithm itself. If it does, it must be in an area where it can affect both direct and inverse referencing in a similar manner. The SGP model would be such a place. This is all speculation for the moment, additional data using other satellites will have to be collected.

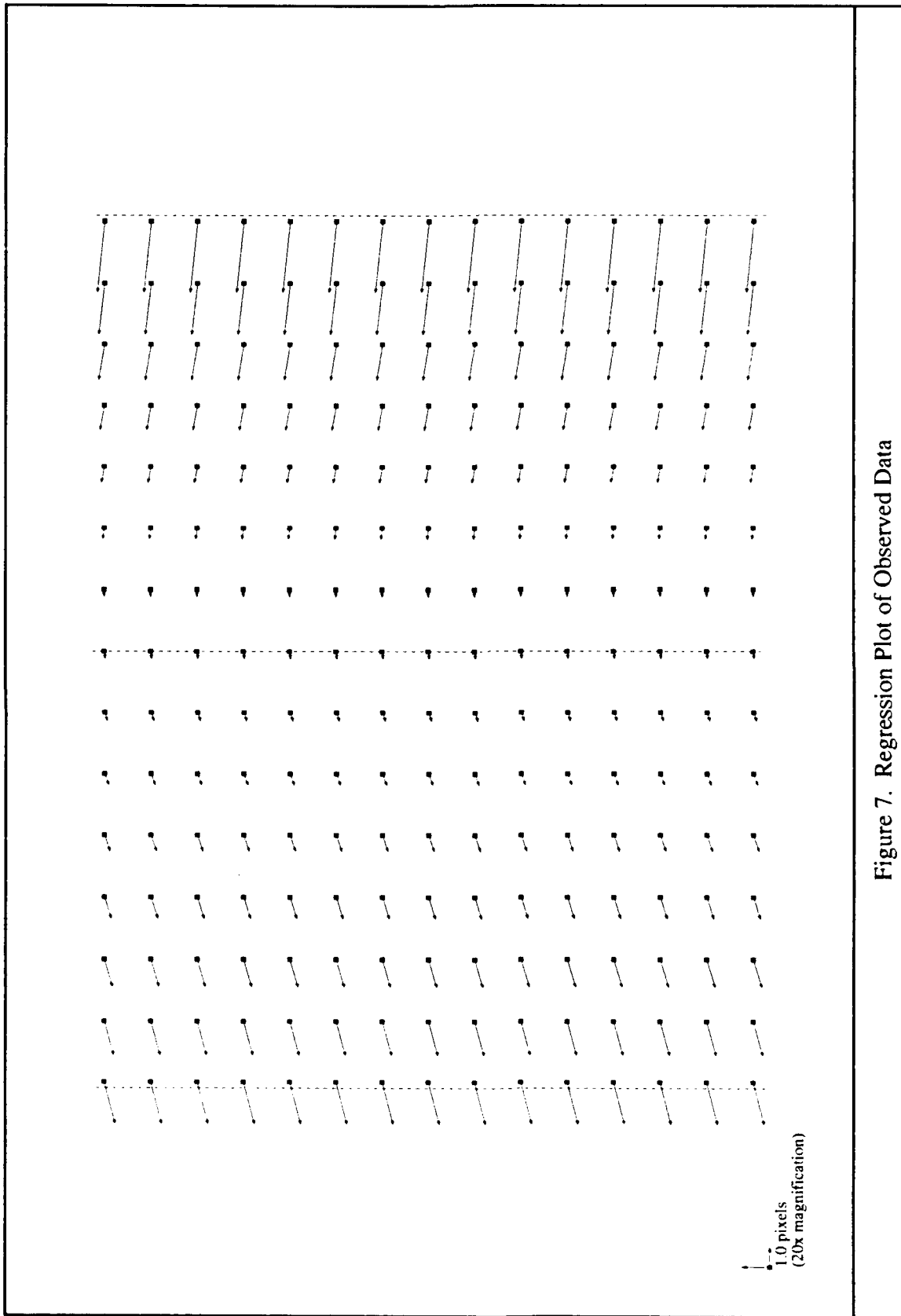


Figure 7. Regression Plot of Observed Data

Sensitivity Analysis

Figures 8 - 16 are predicted error fields for various conditions. The errors are plotted in an APT coordinate frame. Errors viewed on a screen will appear in a similar manner. Some errors, such as attitude control problems or timing problems behave independently of the position of the satellite. Other errors, such as inclination error, have a strong dependence on latitude. The examples shown are at 40 degrees north. The first plot of the series depicts no errors and is included to show the initial array of points used in the tests.

Figures 9, 10, and 11 depict attitude control problems. Normally, spacecraft attitude is kept within ± 0.12 degrees of planned, with only brief anomalies up to ± 0.2 degrees [3:18]. The figures depict attitude errors of 3 degrees in order to more clearly show their effects.

An image of special interest is Figure 17. This image was received on 31 July 1990. A map outline containing coastal features was overlayed. The registration error pattern suggests that the satellite experienced a -0.8 degree yaw deviation. These errors have been reported to have occurred on the NOAA 11 satellite intermittently during this period. An attitude control engineer at General Electric Government Services confirmed that the satellite experienced a yaw anomaly of -0.9 degrees on this date.

According to the engineer, this was the first time a user has identified an attitude control problem to their office.

It was explained that the yaw anomaly occurs when an attitude correction is made after the onboard computer resets its yaw bias model. The deviation normally begins during the orbit that follows the bias reset and remains for one or two additional orbits. This creates a vulnerability window in which images will show the effects of yaw. The yaw bias reset event on 31 July occurred at 14:06 UTC. The vulnerability window extended from shortly after this until roughly 18:30 UTC. The image was received at 18:08, which would place it inside the window.

General Electric began to track the yaw problem on 19 July 1990. Unfortunately, this was only two weeks before the end of the data collection period for this thesis. For the days from 19 July to 5 August 1990, no other images were received during known yaw problem vulnerability windows. An inspection of the images for these days showed no signs of yaw error except for the one on 31 July. The 31 July image was captured during a yaw vulnerability window. Therefore, there is a strong correlation between known yaw anomalies and observed registration errors. As was mentioned earlier, several other pictures suggested yaw problems, but these were captured before 19 July, and therefore cannot be correlated with known anomalies.

Figure 12 depicts an error of the reported mean motion. The net effect of the error can be interpreted as being

twofold. The along-track displacement is because of the timing problem since the spacecraft is traveling with a different orbital period than expected. The cross-track error is because of a difference in altitude, since orbital radius is a function of orbital period. The resulting difference in altitude results in errors in the scan angle calculation. The effect is the same as that described in Chapter III, under the discussion on inverse referencing.

Referencing does not appear to be very sensitive to errors in eccentricity. The error depicted is 4 times the nominal value. The magnitude of this error depends on which portion of the orbit the satellite is in during the pass (see Figure 13).

Two effects caused by ascending node error are evident in Figure 14. The overall cross-track error is the result of displacing the satellite east or west as it crosses the equator. The along-track error is caused by an error in the scan line computation. This error is inversely proportional to the distance that the earth point lies from the satellite ground track.

Errors in inclination show a combination of effects. One effect, a general displacement to the west or east, is a function of the latitude of the scan lines. The other effect is a twisting of the scan lines. This twist has its greatest impact at the edges of the swath (see Figure 15).

Figure 16 depicts registration with incorrect image time. The error is restricted to the along-track direction.

Errors in the satellite epoch, and the argument of perigee
will have a similar registration error pattern.

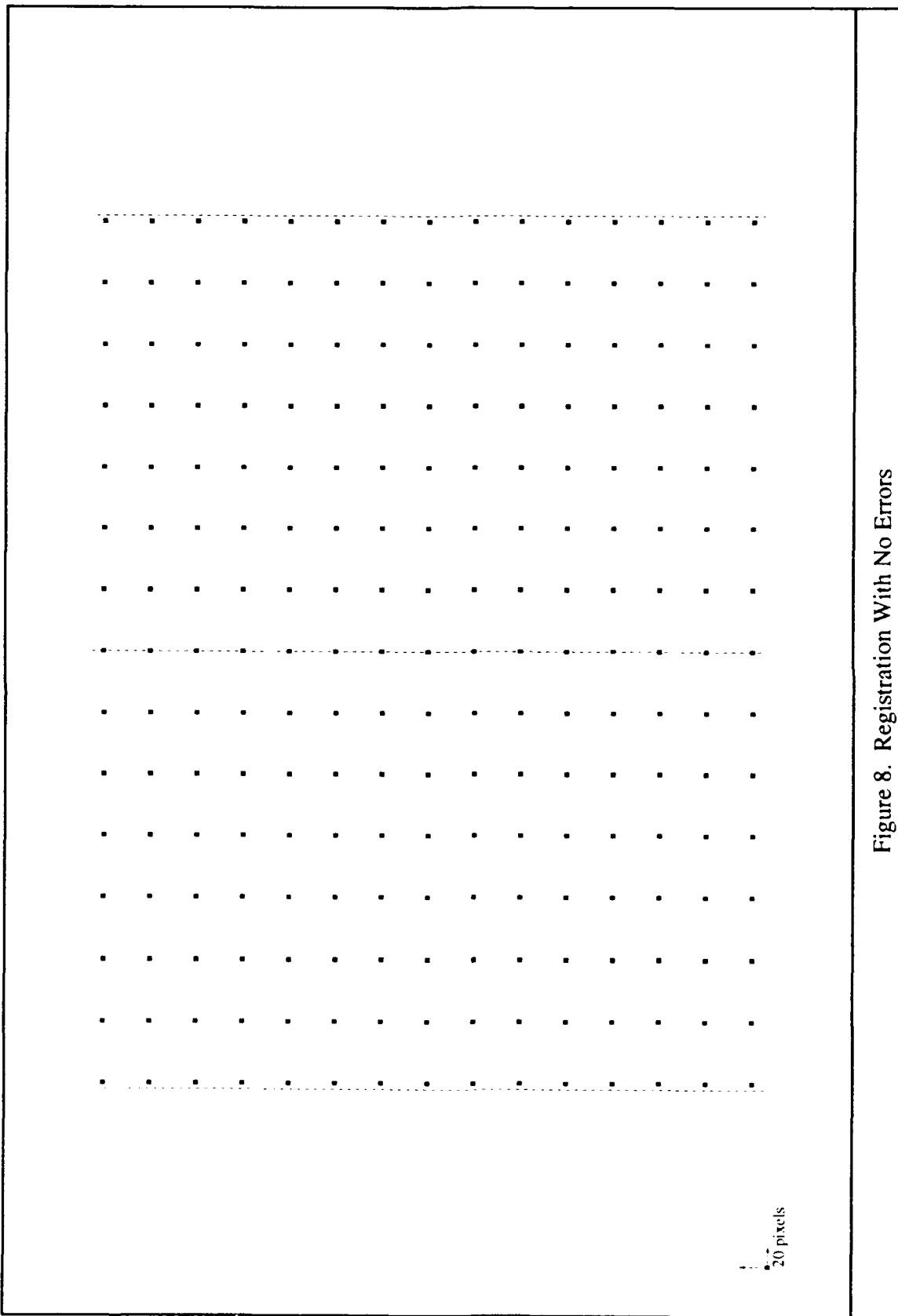


Figure 8. Registration With No Errors

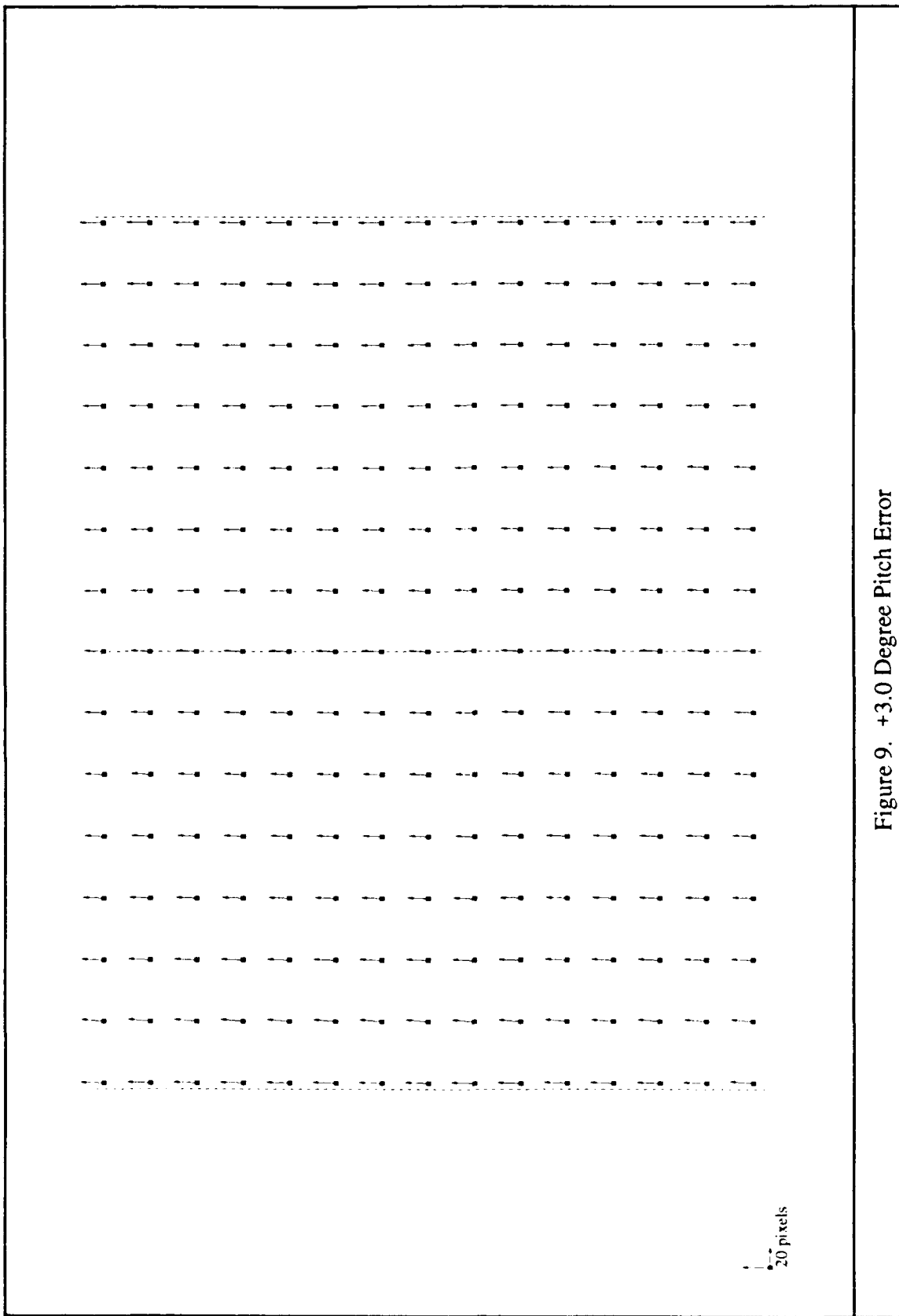


Figure 9. +3.0 Degree Pitch Error

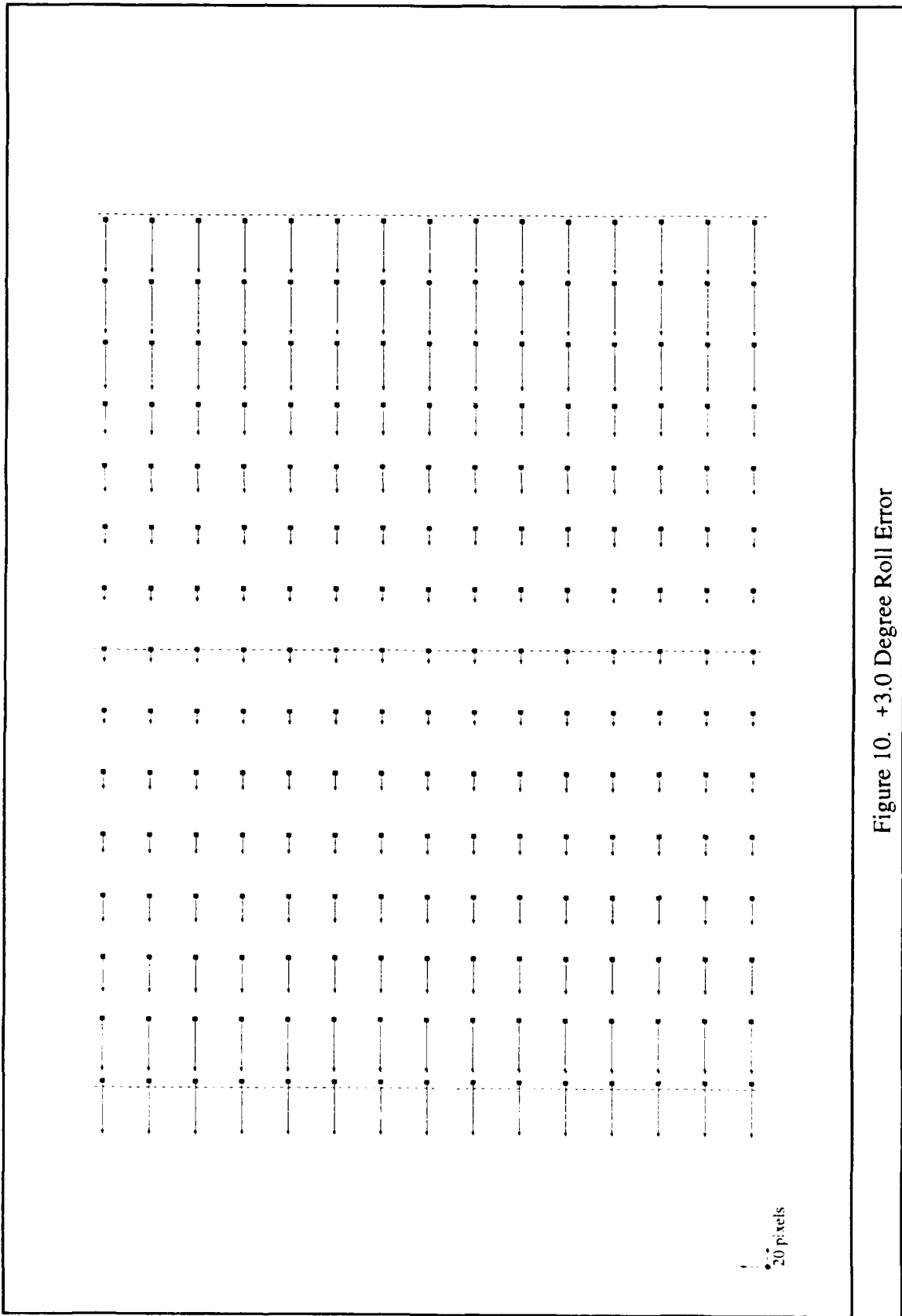
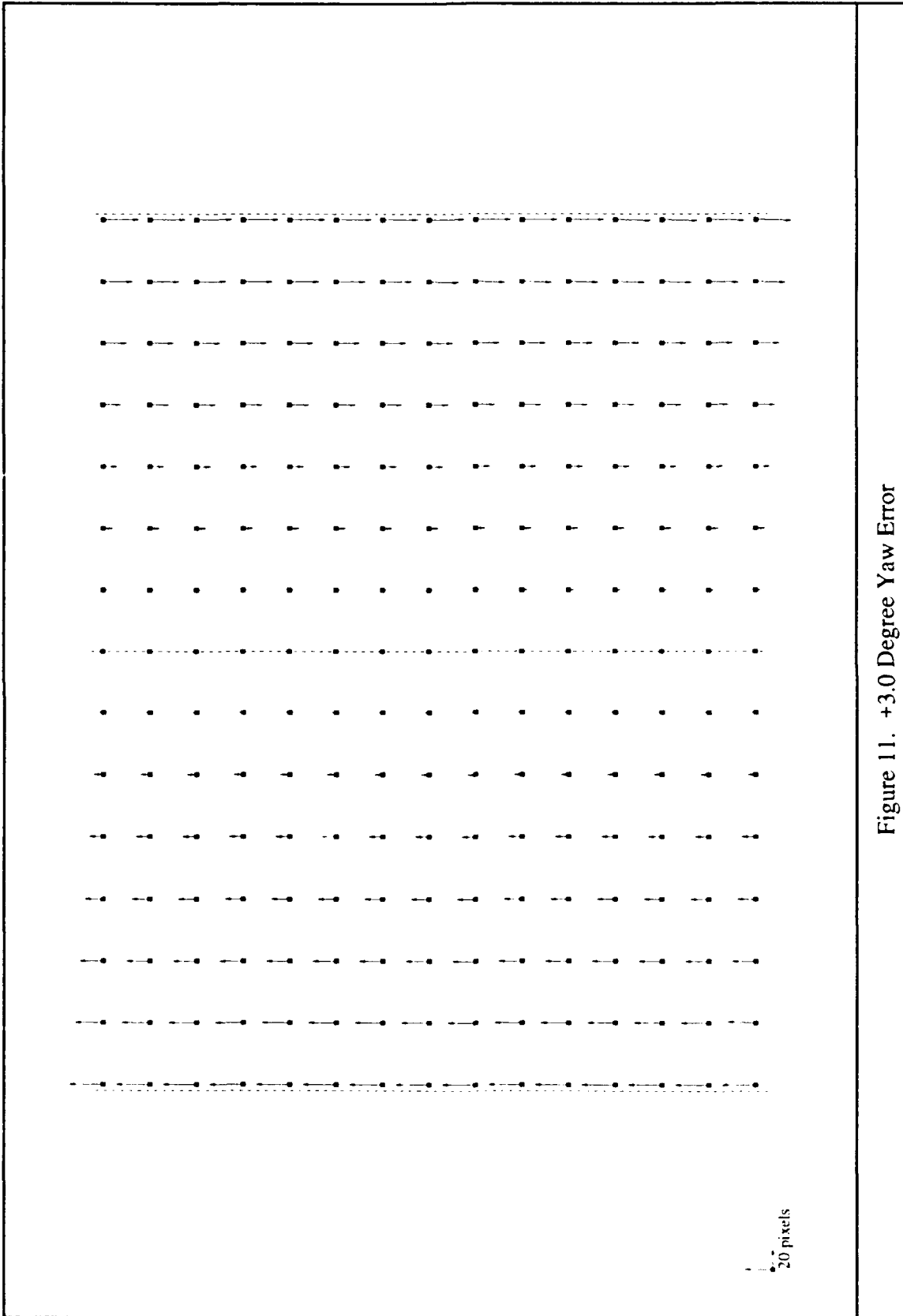


Figure 10. +3.0 Degree Roll Error



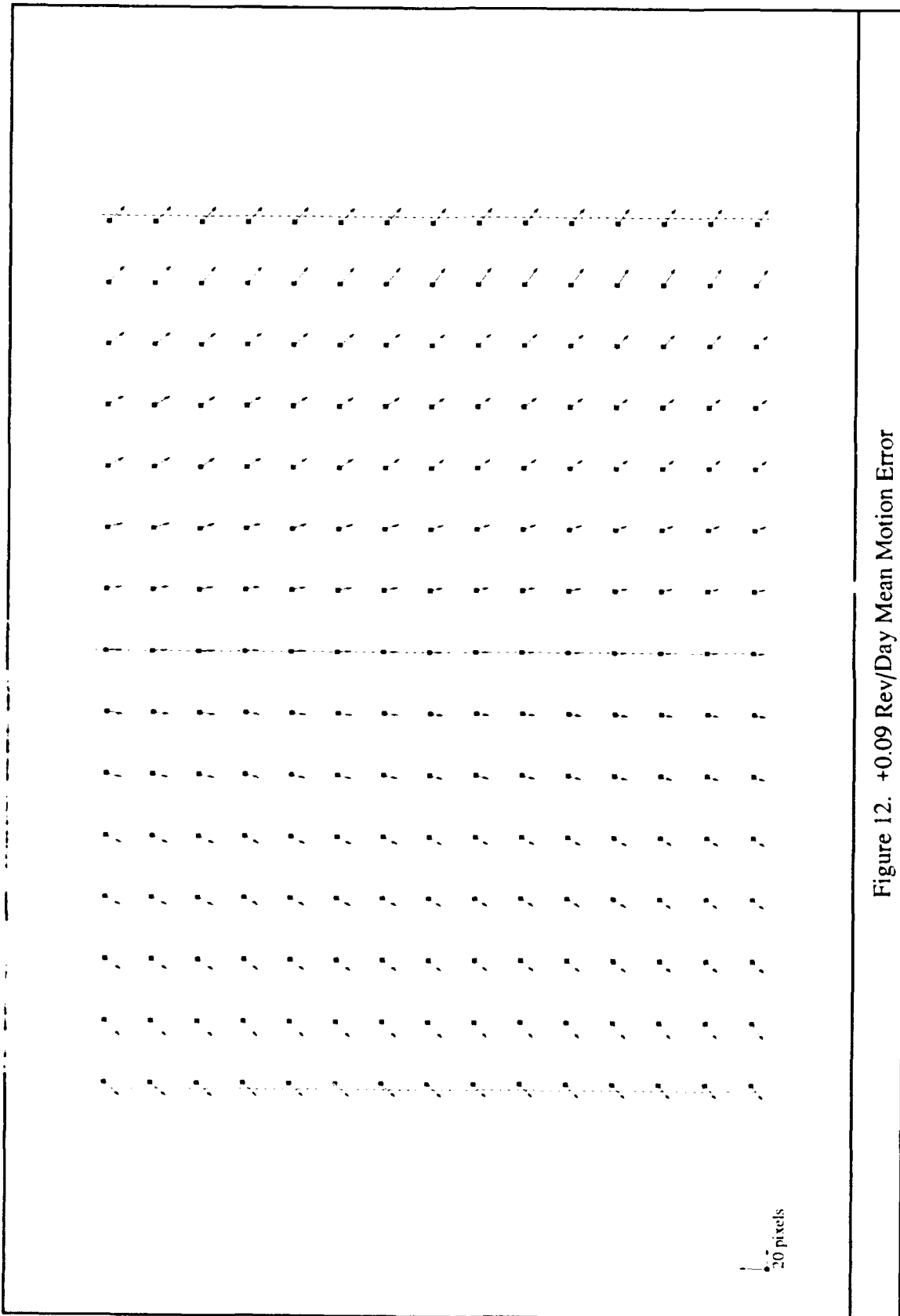
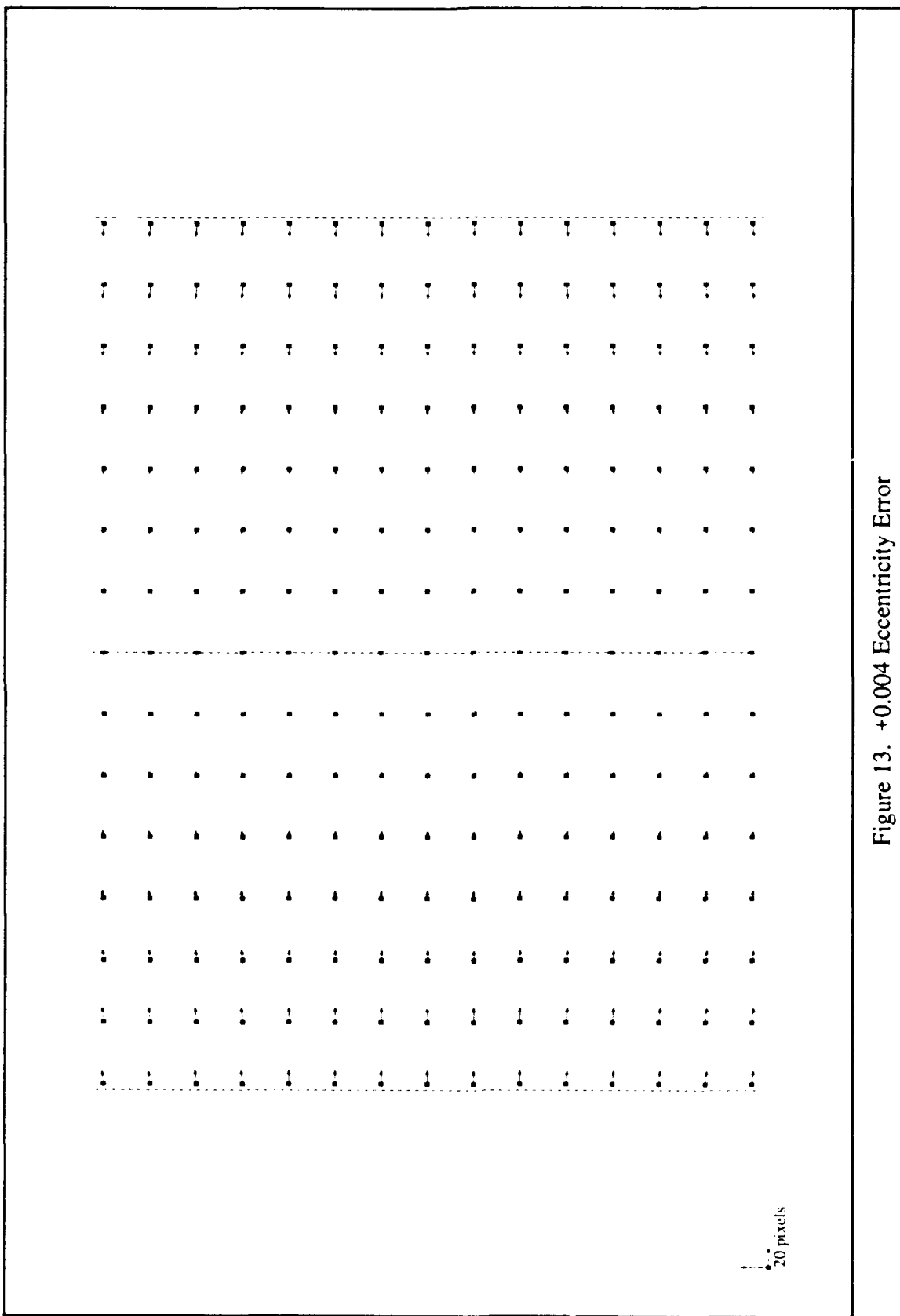


Figure 12. +0.09 Rev/Day Mean Motion Error



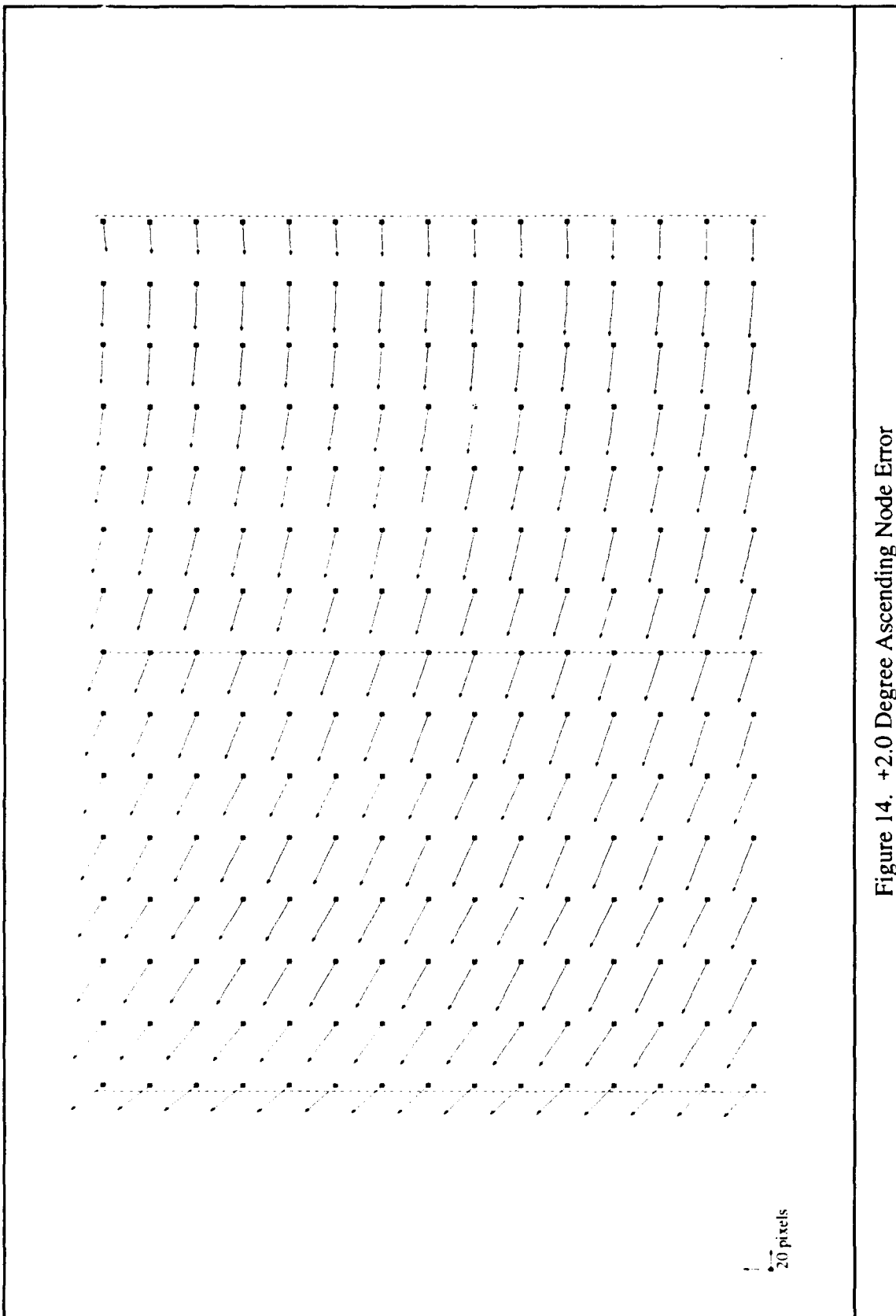


Figure 14. +2.0 Degree Ascending Node Error

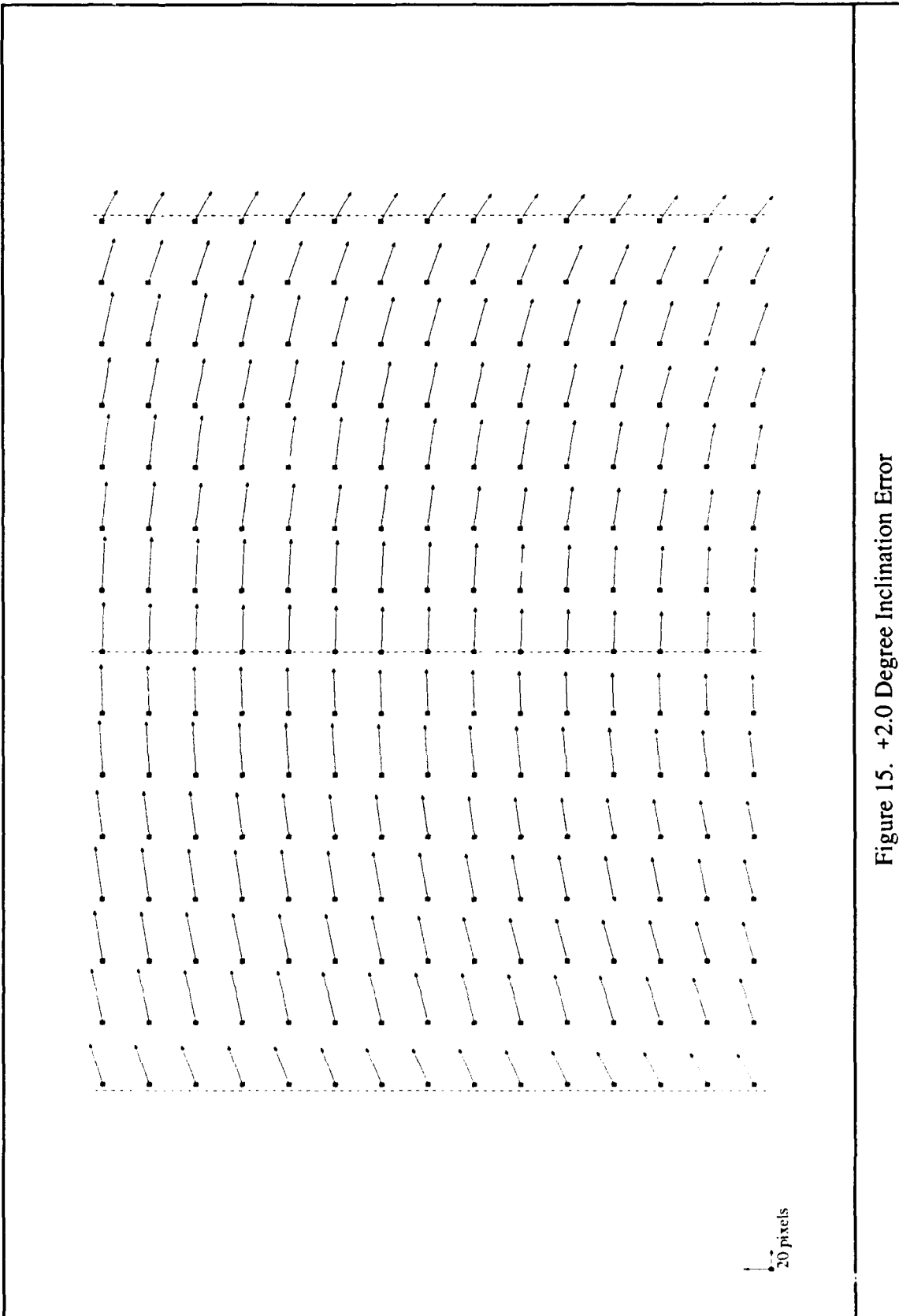


Figure 15. +2.0 Degree Inclination Error

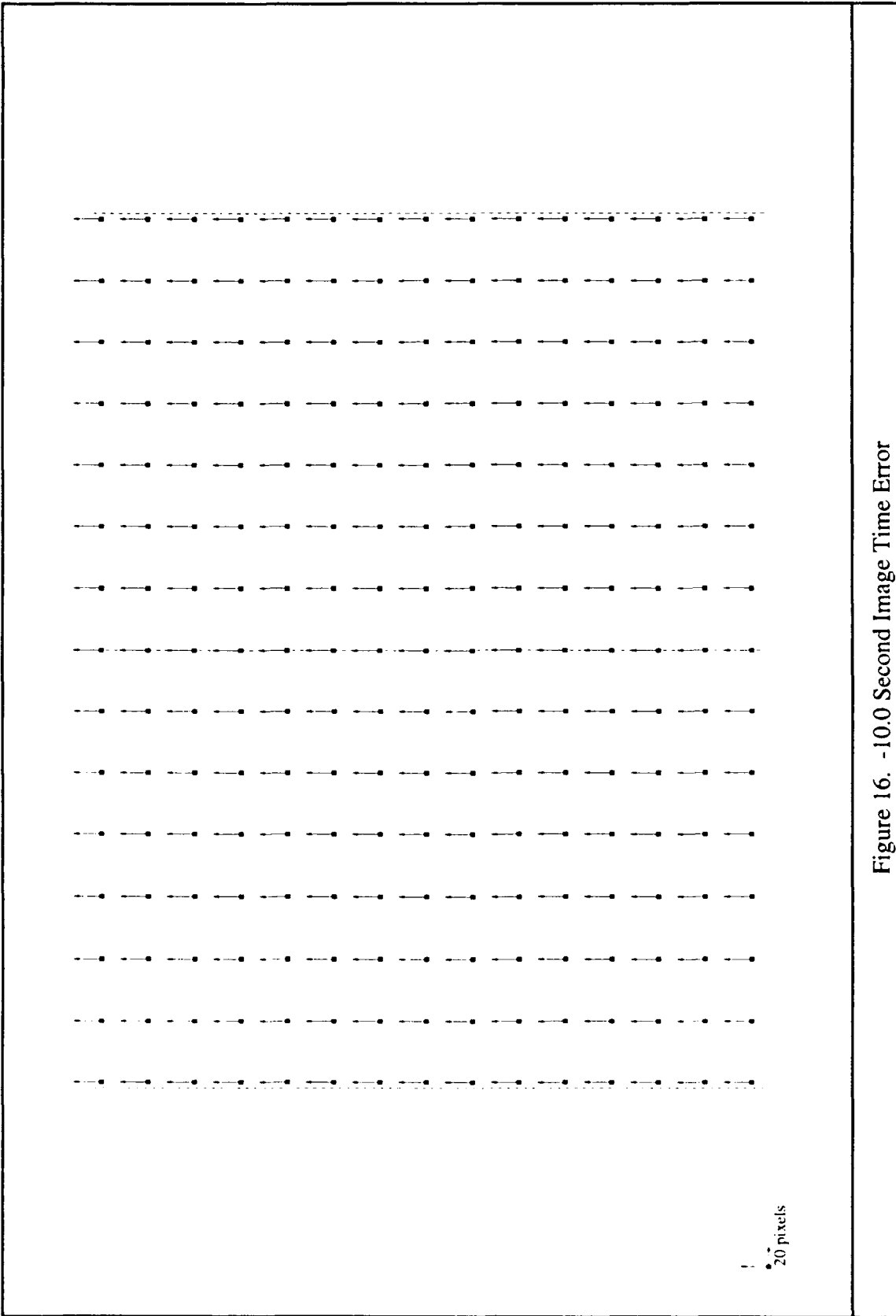


Figure 16. -10.0 Second Image Time Error

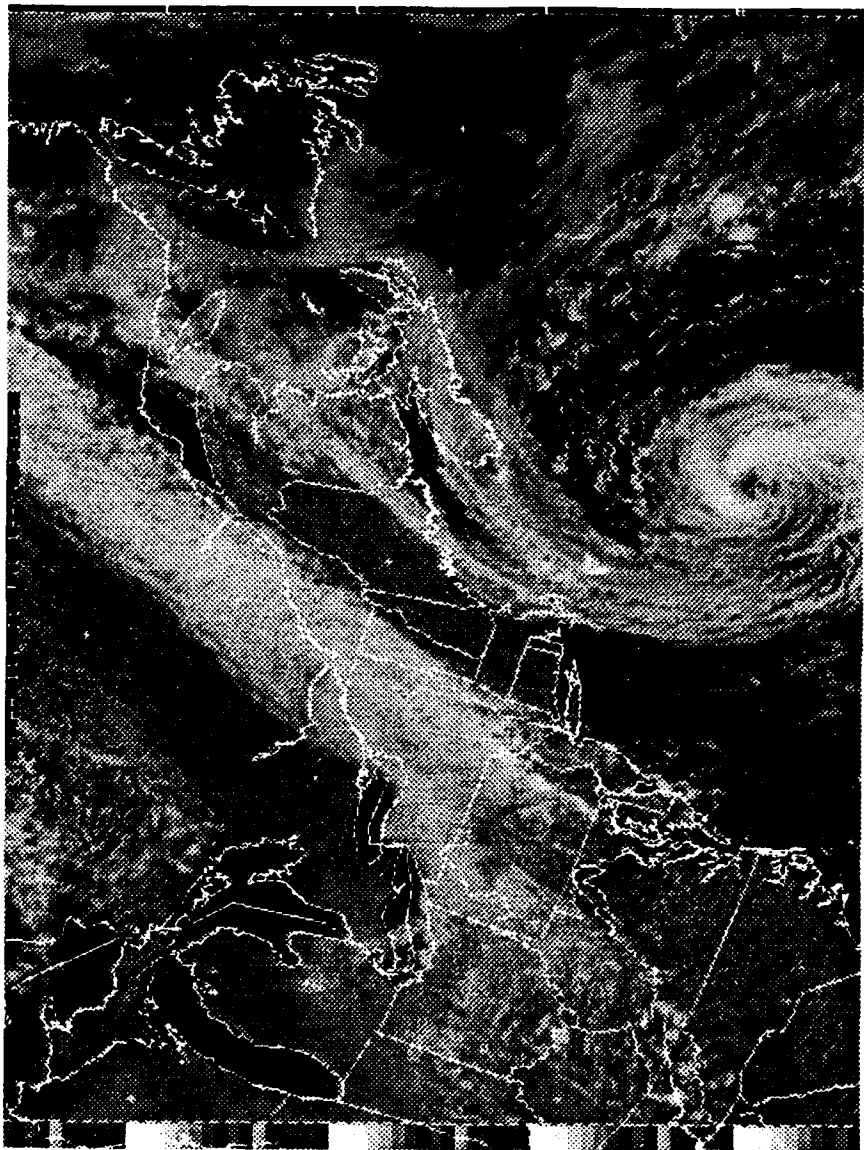


Figure 17. Registered Image With Satellite Yaw Error

VI. Conclusions and Recommendations

Conclusions

Registration of TIROS-N satellite images on personal computers based on precise timing and orbital data is now a working technique. The algorithm proposed by Larcomb has been translated into a structured programming environment, making it workable with a variety of systems.

This thesis had originally attempted to measure the accuracy of the algorithm itself. This goal was only partially obtained because of the attitude control and minute mark problems. Instead, it has turned out to be a measurement of how the algorithm might perform under normal, day-to-day operations. The resulting accuracy of 1.6 APT pixels is almost invisible to the naked eye on high-resolution monitors. Applications, such as the charting of ocean currents, have a new source of high precision measurement. APT infrared images can soon be used with confidence. APT multispectral imaging may be the beginning of low-cost earth resources operations.

The algorithm's sensitivity to errors has been shown by simulation and in practice. Errors in orbit, data or attitude control can produce recognizable patterns of errors. These patterns can sometimes be used to identify the source of errors.

One notable error is the -0.88 pixel cross-track error. While several candidate causes are suspected, the true cause remains to be identified. Since this error is the largest overall error, its cause and correction is a high priority. Eliminating it will reduce registration errors to near zero. Additional data will have to be collected before such an attempt is made. Registration data from NOAA 9 and NOAA 10 might be helpful in identify the cause.

The successful identification of a satellite yaw anomaly underscores the accuracy and precision of the technique. Statistical monitoring of satellite data can result in valid conclusion regarding the condition of satellite systems and their operation.

Recommendations

This thesis has demonstrated the accuracy, precision, and reliability of the registration technique. Still, there is room for improvement. Some areas of research may include:

1. Test and validate the algorithm with the NOAA 9 and NOAA 10 satellites.
2. Test and validate NOAA's new minute mark update procedure. Establish if the along-track accuracy measurements are valid for the new procedure.
3. Identify and correct, if possible, the cause of the -0.88 pixel cross-track error. If error cannot be identified, devise a fix based on the regression analysis.
4. Test and validate the algorithm for infrared images.
5. Extend the algorithm to other polar-orbiting spacecraft such as the Defense Meteorological Support Program (DMSP) satellite and the Soviet Union's Meteor-series satellites.

Appendix A: Ref Unit

The following is the interface section of the referencing unit. This unit uses the Simplified General Perturbation Model and the Math Library units. No decision has been made regarding the release of the source code at this time. It is hoped that a compiled form of this unit will be made available in the near future.

Unit Ref;
{\$N+}

| This unit accomplishes geographical registration of APT data from NOAA TIROS-N meteorological satellites. This unit must be initialized prior to the first call to either the direct or inverse referencing procedures. It also must be called again prior to registering another image. To initialize call: Reference_Initialize(. . .) passing the following data:

ElSetFile	-	The name of a file of NORAD 2-line element sets.
SatNum	-	The NORAD satellite number, i.e. '19531'.
ImageEpoch	-	The date of image receipt, i.e. 90025, the 25th day of 1990.
ImageTime	-	The UTC time of image receipt in minutes.
APTChannel	-	The APT channel to be registered.

Registration can be done in either of two ways. Direct referencing will calculate a latitude/longitude for a given APT line and pixel (column). The line and pixel coordinates must correspond to the location of the data transmitted by the satellite, independent of how it was received. See the unit called 'APT_RST' for conversion routines. The lat/lon returned is in radians, with North and East set to positive, South and West set to negative.

Inverse referencing calculates an APT line and pixel when provide a lat/lon pair. The above conventions apply.

The procedure SetNudgeTime has been added to allow programs to alter the time used in registration calculations. The default nudge time is zero. Use SetNudgeTime to change the effective value of the image time without having to reinitialize the ref unit. Warning: Initialization does not

reset the nudge time to zero. If the nudge time is changed at any time during operation, the change will remain in effect until the nudge time is reset to zero by using the SetNudgeTime procedure. A positive value has the effect of making the image time later. The function GetNudgeTime returns the current value of the nudge time. The value returned is real.)

Interface

Uses

```
MathLib,SGPModel,GraphHRZ,APT_CRT;

procedure Reference_Initialize(ElSetFile : string; SatNum : string;
                               ImageEpoch : double; ImageTime : real;
                               IAPTChannel : char; SearchMode : integer);
procedure Direct_Reference(line,pixel:real; var MapLat,MapLon:real);
procedure Inverse_Reference(MapLat,MapLon:real; var x,y:real);
procedure SetNudgeTime(newtime : real);
function GetNudgeTime : real;
```

Appendix B: Support Unit

The following is the interface section of the APT to CRT conversion unit. No decision has been made regarding the release of the source code at this time. It is hoped that a compiled form of this unit will be made available in the near future. Note, since this routine is machine specific, a Video 7 VGA card with 512K memory is required to use this unit. A user-written unit can be substituted when other hardware is used.

Unit APT_CRT;

{ This unit contains functions to convert APT coordinates to simple screen coordinates. A one-to-one correspondence between screen pixels and file bytes is assumed (ie. no particular projection is displayed). This unit must be initialized before any of the functions are called. To initialize the unit call APT_CRT_Initialize(. . .) with the following parameters:

APTDataRate	- Data transmission rate, normally 4160 words/sec.
SampleRate	- Data capture rate, a function of capture method.
ReductionRatio	- Adjustment for when a fraction of the data is disposed of during data storage to reduce file space.
OffsetX	- Number of captured bytes at the beginning of a line that do not include raster data (sync and telemetry for example).
OffsetY	- Number of lines in file that are to be skipped. (Note: APT line numbers are relative to the first line in the captured file.)
Pass	- Must be set to the predefined value of - Ascending or Descending, as appropriate.

To convert from one coordinate to the other just call the appropriate function with corresponding parameter.)

Interface

```
type
  PassType = (Ascending, Descending);

procedure APT_CRT_Initialize(IAPTDATArate, ISampleRate, IReductionRatio : real;
                           IOffsetX, IOffsetY : integer; Pass : PassType );
function APTpixel(x : integer) : real;
function APTline(y : integer) : real;
function CRTpixel(x : real) : integer;
function CRTline(y : real) : integer;
```

The following is the interface section of the APT-to-RST file format conversion unit. No decision has been made regarding the release of the source code at this time.

Note, this routine is machine specific, an A & M Design Weather Satellite Interface system for capturing images is required to use this unit. A user-written unit can be substituted when other hardware is used.

Unit APT_RST;

{ This unit contains functions to convert APT coordinates to a RST data file format. Inverse functions are also provided. This unit be initialized before any of the functions are called. To initialize the unit call APT_RST_Initialize(. . .) with the following parameters:

APTDATArate	- Data transmission rate, normally 4160 words/sec.
SampleRate	- Capture data rate, a function of capture method.
ReductionRatio	- Adjustment for when a fraction of the data is disposed of during data storage to reduce file space.
OffsetX	- Number of captured bytes at the beginning of a line that does not include raster data (sync and telemetry for example).
OffsetY	- Number of lines (groups of PixelsPerLine) in file that are to be skipped.
PixelsPerLine	- The number of bytes in the file that corresponds to one scan line of data.

To convert from one coordinate to the other just call the appropriate function with corresponding parameters.}

Interface

```
procedure APT_RST_Initialize(IAPTDataRate,ISampleRate,IReductionRatio : real;
                           IOffsetX, IOffsetY, IPixelsPerLine : integer);
function RSTtoAPTpixel(p : integer) : real;
function RSTtoAPTline(l : integer) : real;
function RSTpixel(p : real) : integer;
function RSTline(l : real) : integer;
```

Appendix C: Verification Test Programs

The following is a fragment from the verification test program. It is included here as an example as to how the modular programming units can be used to accomplish image registration. Other examples have been added which demonstrate some useful techniques which could be applied to map outlining and gridding. It should be noted how few statements are needed in order to accomplish registration this way. As can be seen in the examples, registration can be useful for many applications in addition to drawing maps and grids.

Ellipses indicate missing code.

...

Uses

```
Crt,Dos,Graph,Ref,APT_CRT,APT_RST;
```

...

```
{All units must be initialized for each image.}
```

```
APT_RST_Initialize(APTDataRate, SampleRate, ReductionRatio, 4, 0, 640);
APT_CRT_Initialize(APTDataRate, SampleRate, ReductionRatio, 4, 0, 1);
Reference_Initialize(ElementsetFileName, SatelliteNumber, ImageEpoch,
                     ImageTime, APTChannel, 0);
```

...

```
{This example will plot a point.}
```

```
Inverse_Reference(lat, lon, aptx, apty);
PutPixel(CRTpixel(aptx), CRTline(apty), PixelColor);
```

```
{This example will compute the geographic location for the center of the
screen.}
```

```
Direct_Reference(APTline(Round(GetMaxY/2), APTpixel(Round(GetMaxX/2)),
    lat, lon);
```

```
    . . .
{This example will retrieve the intensity value of a geographic location
from the data file - useful for special map projections and
surveillance.}
```

```
Inverse_Reference(lat, lon, aptx, apty);
seek(infile, APTtoRST(apty, aptx);
read(infile, PixelIntensity);
```

```
    . . .
{This is an example of the verification test routine simplified to show
the important elements.}
```

```
Direct_Reference(Linel,Pixell,Lat1,Lon1);
Inverse_Reference(Lat1,Lon1,Pixel2,Line2);
LineError = Line2 - Linel;
PixelError = Pixel2 - Pixell;

{plot the error}
circle(Pixell,Linel,radius);
moveto(Pixell,Linel);
lineref(PixelError * Multiplier, LineError * Multiplier);
```

```
{This procedure will draw the swath limits on the screen. Note, no
referencing is needed, only the conversion from APT coordinates to screen
coordinates.}
```

```
procedure Draw_Swath;
begin
  SetColor(SwathColor);
  Line(CRTpixel(0),0,CRTpixel(0),GetMaxY);
  Line(CRTpixel(455),0,CRTpixel(455),GetMaxY);
  Line(CRTpixel(908),0,CRTpixel(908),GetMaxY);
end; {Draw_Swath}
```

Appendix D: APT-RVW2

APT-RVW2 is a complete program written by Dr. T. S. Kelso. It is currently in the latter stages of development. This program served as the main section of the validation program used by the author. File management, data display, and palette control are functions provided by the main program section. This program utilized the referencing and the APT-to-CRT conversion units for image registration. Utilizing these units, APT-RVW2 can grid images and draw maps without the need of GCPs. Additional features include: selectable screen resolution, data reduction, inverted images (adjustment for pass direction), zoom, and point labeling with latitude/longitude. Figures 4, 5, and 17 are printed from images displayed and registered by this program.

Bibliography

1. Cordan, Ernest W. Jr. and Benjamin W. Patz. "An Image Registration Algorithm Using Sampled Binary Correlation," Proceedings of the IEEE 5th International Symposium on Machine Processing of Remotely Sensed Data. 202-205 New York: IEEE Press, 1979.
2. Dominowski, Roger L. Research Methods. Englewood Cliffs: Prentice-Hall Inc., 1980.
3. Larcomb Capt Charles H. Spatial Registration of TIROS-N Weather Satellite Data. MS Thesis AFIT/GSO/ENS/89D-10. School of Engineering, Air Force Institute of Technology (AU), Wright-Patterson AFB OH, December 1989.
4. Mandel, John. The Statistical Analysis of Experimental Data. New York: Interscience Publishers, 1964.
5. Popta, R.G. van. On-Line Superposition of Geographical Data to TIROS-N Type Meteorological Satellite Images. Amsterdam: National Aerospace Laboratory, 1982 (AD-B094 779).
6. Smith, Mona. APT Information Note 90-2. Monthly Newsletter. NOAA/NESDIS Direct Readout Staff, Washington: U. S. Department of Commerce, 1990.
7. Sun, Weidong and Mikio Takagi. "Geometric Distortion Correction with High Accuracy for NOAA Satellite Images," Digest of the IEEE International Geoscience and Remote Sensing Symposium. 1257-1262. New York: IEEE Press, 1987.
8. Tozanwa, Y. "Fast Geometric Correction of NOAA AVHRR," Proceedings of the IEEE 9th International Symposium on Machine Processing of Remotely Sensed Data. 46-53 New York: IEEE Press, 1983.

Vita

Captain Jerry L. Mehlberg

In 1974 he joined the Army. While in the Army, then a warrant officer, he piloted helicopters for a medical evacuation unit and a field artillery unit. While serving in the Army, he received an associate degree from Northwestern State University of Louisiana. In 1978, he left the Army to pursue a bachelor of science degree in Applied Mathematics, Engineering, and Physics at the University of Wisconsin in Madison. Receiving his commission through the ROTC, he began Air Force flight school in 1981. Since then, he has flown F-4 and KC-135 aircraft. In 1989, he started graduate study at the Air Force Institute of Technology majoring in Space Operations.

REPORT DOCUMENTATION PAGE

Form Approved
OMB No. 0704-0188

Public reporting burden for this collection of information is estimated to average 1 hour per response, including the time for reviewing instructions, searching existing data sources, gathering and maintaining the data needed, and completing and reviewing the collection of information. Send comments regarding this burden estimate or any other aspect of this collection of information, including suggestions for reducing this burden, to Washington Headquarters Services, Directorate for Information Operations and Reports, 1215 Jefferson Davis Highway, Suite 1204, Arlington, VA 22202-4302, and to the Office of Management and Budget, Paperwork Reduction Project (0704-0188), Washington, DC 20503.

1. AGENCY USE ONLY (Leave blank)	2. REPORT DATE	3. REPORT TYPE AND DATES COVERED	
	5 Dec 90	MS Thesis: July - December 1990	
4. TITLE AND SUBTITLE Development of an Image Registration Technique for Polar-Orbiting Satellites		5. FUNDING NUMBERS	
6. AUTHOR(S) Jerry L. Mehlberg Captain, USAF			
7. PERFORMING ORGANIZATION NAME(S) AND ADDRESS(ES) Air Force Institute of Technology Wright-Patterson AFB, Ohio		8. PERFORMING ORGANIZATION REPORT NUMBER AFIT/GSO/ENS/90D-12	
9. SPONSORING/MONITORING AGENCY NAME(S) AND ADDRESS(ES)		10. SPONSORING/MONITORING AGENCY REPORT NUMBER	
11. SUPPLEMENTARY NOTES Thesis Advisor: Kelso, Thomas S., Major, USAF			
12a. DISTRIBUTION/AVAILABILITY STATEMENT Distribution unlimited		12b. DISTRIBUTION CODE	
13. ABSTRACT (Maximum 200 words) In this study, a means to perform spatial registration (gridding) of meteorological satellite data is developed. It is applicable to Automatic Picture Transmission (APT) data from the TIROS-N series polar-orbiting satellites operated by the National Oceanic and Atmospheric Administration (NOAA). This technique does not require the use of ground control points. Registration is accomplished using an advanced orbital model to precisely compute the satellite's location based on NORAD two-line element sets and the time of the image. This technique is examined for accuracy and sensitivity to errors in the element set and satellite attitude control. This study involves over 70 images over a 60-day period.			
14. SUBJECT TERMS Image Registration Space Science Meteorological Satellites, Artificial Satellites		15. NUMBER OF PAGES 90	
		16. PRICE CODE	
17. SECURITY CLASSIFICATION OF REPORT UNCLASSIFIED	18. SECURITY CLASSIFICATION OF THIS PAGE UNCLASSIFIED	19. SECURITY CLASSIFICATION OF ABSTRACT UNCLASSIFIED	20. LIMITATION OF ABSTRACT UL